

RESUMENES POSTER

PONENTE	TITULO Y AUTORES	
Alberca	Ferromagnetic Resonance of La_{0.7}Ca_{0.3}MnO₃ ultrathin films on BaTiO₃ ferroelectric substrates A. Alberca, N. M. Nemes, F.J. Mompean M. García-Hernandez, J. Tornos, C. Leon, J. Santamaria, Titusz Fehér, Ferenc Simon	P-01
Alvarez R.	Interpretation of eRBS spectra for H quantification at surfaces. R. Álvarez,* K. Tokesi, F. Yubero	P-02
Antón C.	Flow dynamics on OPO-polariton condensates C. Antón, * G. Tosi, A. Lemaître, J. Bloch, M.D. Martin and L. Viña	P-03
Awad	Double vortex dynamics in vertically coupled Permalloy dots A. A. Awad*, A. Lara, M. García Hernández, V. Metlushko, and F. G. Aliev	P-04
B. del Rosal	Optical activation of BaMgF ultra-transparent ferroelectric crystal B. del Rosal*, P. Molina, M.O Ramírez, E.G Villora, K. Shimamura and L.E. Bausá	P-05
Baena	Electrical control of donor electrons in Si: valley composition and consequences for quantum computing. A. Baena*, A. Saraiva, B. Koiller, and M.J. Calderón	P-06
Bartolomé	Magnetism and structure of amorphous Co-W alloyed nanoparticles A. I. Figueroa, C. Magén, A. Ibarra, L. Ruiz, J. M. González-Calbet, F. Petroff, C. Deranlot, S. Pascarelli, P. Bencok, N. B. Brookes, F. Wilhelm, A. Rogalev, F. Bartolomé*, L. M. García, and J. Bartolomé.	P-07
Blázquez	Transferencia de energía en los molinos planetarios J. S. Blázquez*, C.F. Conde, A. Conde	P-08
Calderón	Magnetic state and anisotropy in the Fe-based high T_c superconductors M.J. Calderón*, B. Valenzuela, and E. Bascones	P-09
Gállardo-López Ángela	Processing and microstructure of spark plasma sintered 8Y-CSZ/5 vol% SWNT composites E. Carrillo*, R. Poyato, A. Gallardo-López, A. Muñoz	P-10
Castro Smirnov	Flexible interference filters for UV radiation shielding applications J.R. Castro Smirnov*, M. E. Calvo and H. Míguez	P-11
Cid	Anisotropic negative thermal expansion in Nd_xCo_{1-x} thin films with perpendicular magnetic anisotropies R. Cid,* J. Díaz, L. M. Álvarez-Prado, R. Morales, J. M. Alameda,	P-12
Cuadra	Coherence of polariton condensates under OPO configuration J. Cuadra*, R. Spano, C. Lingg, M.D. Martin, L. Viña, D. Sanvitto†, M. van der Poel and J.M. Hvam	P-13
Delgado	Probing the nuclear spin of a single donor in Silicon nanotransistors. F. Delgado,* and J. Fernandez-Rossier	P-14
Francisque	Characterization of metallic nanocontact shape by electron-phonon interaction T. Francisque*, C. Sabater, G. Saenz-Arce, C. Untiedt	P-17
García del Muro	The effect of microstructure and interactions in the effective energy barrier distribution of granular Co-Zirconia films M. García del Muro,* Z. Konstantinović, X. Batlle and A. Labarta	P-18
García-Aldea	Efecto de Haas van Alphen y Ceros de Spin en YBCO David García-Aldea,* Sudip Chakravarty	P-19
González J. M.	Hysteresis and radiofrequency absorption behavior in epitaxial Au/Fe/Au/Fe/MgO films M. Iglesias, E. Paz, F. J. Palomares, F. Cebollada, J. M. González and N. Sobolev	P-21
Hierro-Rodríguez	Confined magnetization state in thickness modulated amorphous NdCo₅ films with perpendicular anisotropy. A.Hierro-Rodríguez,* R.Cid, G.Rodríguez-Rodríguez, M.Vélez, J.I.Martín, L.M.Álvarez-Prado, and J.M.Alameda,	P-22
López-López Carmen	Photonic Crystals for Enhanced Light Harvesting in Dye Solar Cells. Carmen López-López,* Silvia Colodrero, and Hernán Míguez	P-24
Luis F.	Molecular Prototypes for Spin-Based CNOT and SWAP Quantum Gates F. Luis,*,* A. Repollés, M. J. Martínez-Pérez, D. Aguilà, O. Roubeau, D. Zueco, P. J. Alonso, M. Evangelisti, A. Camón, J. Sesé, L. A. Barrios, and G. Aromí	P-26
Martínez B. (1)	Transport properties across LaAlO₃/La₂/3Sr₁/3MnO₃ (LAO/LSMO) interfaces R. Galceran, L. Peña, A. Pomar, Z. Konstantinović, B. Bozzo Ll. Balcells, F. Sandiumenge and B. Martínez	P-28
Martínez B. (2)	Interfacial effects in manganite thin films with different capping layers Z. Konstantinovic, R. Galceran, A. Pomar Ll. Balcells, F. Sandiumenge and B. Martínez	P-29

Milan D.C.	Fabrication and Characterization of folded Graphene on Graphite D.C. Milan*, G. Saenz-Arce, M. Moaied, M.J. Caturla, J.J. Palacios & C. Untiedt	P-30
Möller	Low temperature optical emission of wurtzite InAs nanowires M. Möller*, M. M. de Lima, Jr., A. Cantarero, T. Chiaramonte, M. A. Cotta, F. Iikawa	P-31
Palau	Incoherent interfaces and local lattice strains in solution-derived YBCO nanocomposites: a novel vortex pinning mechanism A. Palau*, Llordés, J. Gázquez, M. Coll, R. Vlad, A. Pomar, J.Arbiol, R.Guzmán, S. Ye, V. Rouco, F. Sandiumenge, S. Ricart, T. Puig, M. Varela, D. Chateigner, G. Deutscher, X. Obradors	P-32
Perez de Lara D.	Vortex lattice motion induced by alternating forces in superconducting magnetic hybrid nanostructures D. Perez de Lara, F. Galvez, M. A. Garcia, E. M. Gonzalez, and J. L. Vicent.	P-33
Pérez	Magnetite nanoparticles with bulk like behaviour N. Pérez*, F. Bartolomé, L.M. García, J. Bartolomé, A.G. Roca, M. P. Morales, C.J. Serna, F. López-Calahorra, A. Labarta, X. Batlle	P-34
Rivas-Murias	Optimization of the thermoelectric figure of merit through the fabrication of composites B. Rivas-Murias*, F. Rivadulla,	P-36
Romero J. J.	Effects of agglomeration on nanoparticles properties studied by confocal Raman microscopy J.J. Romero*, I. Lorite, A. del Campo, J.F. Fernandez	P-37
Rouco	Vortex dynamics in YBCO films with engineered antidots and ferromagnetic nanostructures V. Rouco*, A. Palau, C. Monton, T. Puig, X. Obradors, G. Via, C. Navau, N. del Valle, A. Sánchez, R. Córdova, J.M. de Teresa	P-38
Salgueiriño	Goethite (α-FeOOH) Nanorods as Suitable Antiferromagnetic Substrates Verónica Salgueiriño*, Rosalía Mariño-Fernández	P-40
Serrano A	Combined surface plasmon resonance and X-ray absorption spectroscopy A. Serrano*, O. Rodríguez de la Fuente, G. R. Castro and M. A. García,	P-41
Soriano	Manganese phthalocyanine on metallic surfaces: From Kondo effect to magnetoresistance. M. Soriano*, J.J. Palacios	P-42
Alcaire, M.	Soft plasma processing of organic nanowires: a route for the fabrication of 1D. M. Alcaire*, J. R. Sanchez-Valencia, F. J. Aparicio, Z. Saghi, J. C. Gonzalez-Gonzalez, A. Barranco, Y. Oulad-Zian, A. R. Gonzalez-Elipe, P. Midgley, J. P. Espinos, P. Groening and A. Borras	P-43
Álvarez R.	Nanostructure of thin films grown by deposition of isotropically distributed gaseous particles at low temperatures R. Álvarez*. P. Romero-Gomez, J. Gil-Rostra, J. Cotrino, F. Yubero, A. Palmero, A. R. Gonzalez-Elipe	P-44
Awad A. A.	High frequency matching effects of superconducting Pb films with magnetic vortex periodic pinning A.A. Awad*, A. Lara, A.V. Silhanek, G.W. Ataklti, V.V. Moshchalkov, F.G. Aliev	P-45
Baltanás J. P.	Spin waves in magnetic-semiconductor superlattices J.P. Baltanás, D. Frustaglia	P-46
Bartolomé F.	Parimagnetism: Strongly Correlated Paramagnetism in RCo₂ M. Bonilla, J. Herrero-Albillos, I. Calvo, A. Figueroa, C. Castán, J. A. Rodríguez- Velamazán, D. Schmitz, E. Weschke, D. Paudyal, V. K. Pecharsky, K. A. Gschneidner Jr., J. Bartolomé, L. M. García, and F. Bartolomé	P-47
Berceanu A. C.	"Dissipation in a coherently driven polariton fluid" A. C. Berceanu, E. Cancellieri, F. Marchetti	P-48
Cascales J. P.	Magnetic inhomogeneities and spin torque studies by low and high frequency noise in sub-100nm magnetic tunnel junctions J.P. Cascales*, D. Herranz, F.G. Aliev, U.Ebels, J. Katine	P-49
López Sancho Pilar	Disorder and Magnetism in Bilayer Graphene E. V. Castro, M. P. López-Sancho, and M. A. H. Vozmediano	P-50
Cros A.	Doping level of GAN:si nanowires studied by C-AFM and photoluminescencer. Mata, J. Martínez-Pastor, B. Daudin, and A. Cros*	P-51
Doblas D.	Efecto magnetocalórico en multicapas Gd/Ti D. Doblas*, V. Franco, A. Conde, A.V. Svalov, G.V. Kurl'yandskaya,	P-52
Fernandes-Silva L. C.	Photoluminescence of Single ZnOTetrapods L. C. Fernandes-Silva*, M. D. Martín, H. P. Van der Meulen, L.Kłopotowski, J. M. Calleja and L. Viña	P-54
Fernández A.	Amorphous SiOxNy thin films with controlled closed porosity and its effects on refractive index and mechanical properties. V. Godinho, T.C. Rojas, A. Fernández*.	P-55

Fernández J. J.	Time Dependent Density Functional Theory total energy calculations using numerical atomic orbitals J.J. Fernández,* , P. García-González, J.E.Alvarellos	P-56
Galvez F.	Interferences and modulation of Surface plasmons in thin metallic films F. Galvez,* and M. A Garcia	P-58
González J. M.	Epitaxial magnetoplasmonic structures exhibiting enhanced surface-plasmon-polariton wave vector magnetic modulation M. Iglesias, E. Ferreiro-Vila, E. Paz, F. J. Palomares, F. Cebollada, J. M. González, G. Armelles, J. M. García-Martín, and A. Cebollada	P-59
Gosálbez-Martínez D.	Study of the transport properties in two dimensional topological insulators in presence of disorder D. Gosálbez-Martínez,* , J. Fernández-Rossier, J.J. Palacios	P-60
Herranz D.	Low frequency noise due to magnetic inhomogeneities in submicron FeCoB/MgO/FeCoB magnetic tunnel junctions D.Herranz, A. Gomez-Ibarlucea, A. Lara, M. Schäfers, G. Reiss, and F.G. Aliev	P-61
Iglesias-Freire O.	MFM characterization of double-vortex metastable state in circular Permalloy dots O. Iglesias-Freire,* , A. Lara, A. Awad, M. Jaafar, V. Metlushko, A. Asenjo and F.G.Aliev	P-62
Ingale B.	Magnetocaloric effect in Fe₇₇Co_{5.5}Ni_{5.5}Zr_{7-z}X_zB₄Cu₁ (X = Nb, Hf) soft magnetic amorphous alloys B. Ingale*, V. Franco, A. Conde, K. E. Knippling, M. A. Willard	P-63
Jiménez-Solano Alberto.	Tailored luminescent emission of dyes embedded in porous resonators Alberto Jiménez-Solano* José Miguel Luque, Mauricio E. Calvo, Fernando Fernández-Lázaro, Hernán Míguez	P-64
Lara A.	Spin waves along domain walls in triangular and circular Py dots with vortices A. Lara,* , A. Awad, F.G. Aliev, V. Metlushko	P-65
Macias-Montero M.	Supported AgNPs@ZnO Nanorods by low temperature PECVDM. Macias-Montero,* , Z. Sagui, A. R. Gonzalez-Elipe, A. Borrás	P-66
Macias-Montero M. (2)	Growth of SiO₂ Thin Films by Plasma-Assisted Reactive Magnetron Sputtering Under the Impingement of Positive and Negative Ions M. Macias-Montero*, F.J. Garcia-Garcia, R. Álvarez, J. Gil-Rostra, F. Yubero, A. R. Gonzalez-Elipe, A. Palmero, J. Cotrino,	P-67
Martín J.I.	Nanoestructuración de Láminas Magnéticas mediante Copolímeros en Bloque Auto-Organizados F. Valdés-Bango, F.J. García Alonso, G. Rodríguez-Rodríguez, L. Morán Fernández, J.I. Martín,* , J.M. Alameda ,	P-68
Mestres Narcís.	Oriented epitaxial growth of ferromagnetic LaSr-2x4 manganese oxide molecular sieve nanowires Adrián Carretero-Genevrié, Jaume Gázquez, César Magén, J. Oró, María Varela, Etienne Ferain, Teresa Puig, Narcís Mestres*, and Xavier Obradors	P-69
Moya C.	Co-ferrite nanoparticles with spin glass-like surface shell C. Moya, N. Pérez, X. Batlle, A. Labarta	P-70
Otero Lorenzo Ruth.	Synthesis of magnetic composites through controlled aggregation of nanoparticles using an autoclave system Ruth Otero Lorenzo,* Sara Liébana Viñas, Verónica Salgueiriño	P-71
Oulad-Zian Y.	Light controlled patterning of ONWs on ITO and TiO₂ Surfaces Oulad-Zian,* J. R. Sanchez-Valencia, A. Borrás, A. R. Gonzalez-Elipe and J. P. Espinos	P-72
Paradinas Markos.	Multi-scale approach correlation between structure and properties Markos Paradinas,* , Mariona Coll, Esther Barrena, Oana D. Jurchescu and Carmen Ocal	P-73
Queraltó A.	Very fast growth of functional oxide thin-films and nanostructures prepared by Chemical Solution Deposition A. Queraltó*, A. Pérez del Pino, T. Puig, X. Obradors	P-74
Romero J.J.	Observation of ferroelectric domains in lead free piezoelectric materials by confocal Raman microscopy J.J. Romero,* , F. Rubio-Marcos, A. del Campo, J.F. Fernandez	P-76
Romero-Muñiz C.	Influencia de las interacciones entre fases en el efecto magnetocalórico de composites C. Romero-Muñiz,* , V. Franco, A. Conde	P-77
Sánchez-Jiménez P.E.	Mechanochemistry as a method for the synthesis of multiferroic materials A.Perejón, P.E. Sánchez-Jiménez,* , M.J. Diánez, J.M. Criado, L.A. Pérez-Maqueda	P-78
Frontera C.	Effect of cationic order and origin of the dielectric anomalies in La₂MnCoO₆. C. Frontera,* , A.J. Barón-González, J.L. García-Muñoz, B. Rivas-Murias, J. Blasco	P-79
Seminóvski Y.	Ab-Initio calculations including Van der Waals interactions: the SnS₂ layered material. Y. Seminóvski, P. Palacios, R. Grau-Crespo, P. Wahnón	P-80

Ferromagnetic Resonance of La_{0.7}Ca_{0.3}MnO₃ ultrathin films on BaTiO₃ ferroelectric substrates

A. Alberca¹, N. M. Nemes¹, F.J. Mompeán¹, M. Garcia-Hernandez¹, J. Tornos², C. Leon², J. Santamaria², Titusz Fehér³, Ferenc Simon³,

¹Instituto de Ciencia de Materiales de Madrid, Consejo Superior de Investigaciones Científicas, Sor Juana Inés de la Cruz, 3, ES-28049 Madrid (Spain)

²Departamento de Física Aplicada III, Universidad Complutense, Ciudad Universitaria, ES-28040 Madrid (Spain)

³Budapest University of Technology and Economics, Institute of Physics, Department of Experimental Physics, H 1521 Budapest (Hungary)

Thin epitaxial films of La_{0.7}Ca_{0.3}MnO₃ grown on ferroelectric BaTiO₃ (LCMO/BTO) display hysteresis loops with extremely unusual features in a limited temperature range, between 40K and 120K: after switching at coercivity, the magnetization overshoots the eventual high-field value. We compare the structural, magnetic and magnetotransport properties of LCMO/BTO with LCMO grown on nonferroelectric SrTiO₃ (LCMO/STO). We study the strains in the film and substrate with x-ray diffraction and propose a model of two magnetic moment populations with different magnetoelastic anisotropies. The relative weights of both populations can be estimated by comparison with LCMO/STO. The temperature dependent resistivity and magnetoresistance also demonstrate the appearance of regions of low conductivity intermixed with the more typical metallic manganite with in-plane moments. FMR results demonstrate that the in-plane easy axis is along (110). Angle dependent ferromagnetic resonance shows that, away from the (110) easy axes, the magnetic domain structure in LCMO/BTO becomes severely fractured where out-of plan and in-plane populations seems to be coupled. This translates into very broad resonances away from the (110) easy axes, that smoothly shift to high field although to a lesser extent than in LCMO/STO case. Away from the easy axis, when the resonance field of the in-plane moments should occur at sufficiently high field values, the two resonances decouple and the out-of-plane spin populations appears isolated in a narrow FMR. We propose that the observed magnetization overshoots are the result from differences in the magnetostriction balance as the applied magnetic field increases. The picture of a nonuniform strain field in La_{0.7}Ca_{0.3}MnO₃ on BaTiO₃, caused by the corrugation of the ferroelectric domains in the rhombohedral phase of BaTiO₃, is compatible with the magnetic granular behavior observed in the temperature and field dependences of the magnetization as well as in the low temperature magnetoresistance exhibited by the epitaxial film.

[1] A. Alberca, N. M. Nemes, F. J. Mompeán, N. Biskup, A. de Andres, C. Munuera, J. Tornos, C. Leon, A. Hernando, P. Ferrer, G. R. Castro, J. Santamaria, and M. Garcia-Hernandez..., Phys. Rev. B **84**, (2011) 134402.

Interpretation of eRBS spectra for H quantification at surfaces

R. Álvarez^{1,*}, K. Tokesi², F. Yubero¹

¹Instituto de Ciencia de Materiales de Sevilla (CSIC – Univ. Sevilla), Sevilla, Spain

²Institute of Nuclear Research of the Hungarian Academy of Sciences (ATOMKI), Debrecen, Hungary

The quantification of H at the surface is a subject of key importance. However, direct quantification of this element at the surface region (<2-3 nm) is not an easy task. Note for example that H does not show photoemission peaks in standard surface analysis by XPS. An indirect way to quantify it is by means of High Resolution Electron Energy Loss Spectroscopy, but only those H atoms participating in the vibrational absorption spectra would be observed. It is also possible H quantification with surface sensitivity by means of Nuclear Reaction Analysis, but this technique is not easily available.

Recently it has been proposed a method (Electron Backscattering spectroscopy, eRBS) to quantify the H content at the surface of a-C:H samples based in the analysis of elastically backreflected electrons with primary energies about 1500 eV [1,2]. It is based on the fact that the recoil energy of the incident electrons depends on the atomic mass of the atoms located at the surface that act as scatter centres. Fairly consistent analysis were found for a-C:H materials and polymer surfaces. [1,2]. This new strategy of analysis has also been use to distinguish between H and deuterium at the surface of ice water [3].

In this presentation we will show a critical interpretation of the measured spectra by help of Monte Carlo simulations. We will show to which extent single and multiple scattering contribute to build a measured spectra, as well as the spatial origin and angular distributions of the signals contributing to the spectra.

[1] F. Yubero et al., Applied Physics Letters 87, 084101 (1-3) (2005)

[2] V.J. Rico et al., Diamond and Related Materials 16, 107-111 (2007)

[3] F. Yubero, K. Tokési, Applied Physics Letters 95, 084101 (3) (2009)

Flow dynamics on OPO-polariton condensates

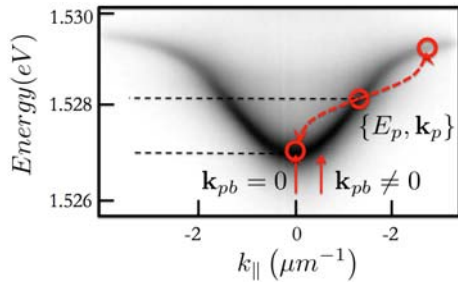
C. Antón,^{1,*} G. Tosi,¹ A. Lemaître,² J. Bloch², M.D. Martin¹ and L. Viña¹¹Física de Materiales, Universidad Autónoma de Madrid, Madrid 28049, Spain²LPN/CNRS, Route de Nozay, Marcoussis 91460, France

Fig 1. Polariton dispersion relation in our sample. Pump laser at $E_p=1.5283$ eV, $k_p=1.4 \mu\text{m}^{-1}$. The solid red arrows depict the two different probe configurations, at $k_{pb}=0$ and $k_{pb}=0.5 \mu\text{m}^{-1}$ close to the OPO-signal energy emission $E_s=1.5268$ eV.

at 10 K and excited with a Ti:Al₂O₃ laser under OPO conditions and probed with a 2 ps-long Gaussian probe, Fig 1.

Observation of quantized vortices in non-equilibrium polariton condensates, suggesting parallels with conventional superfluids, have been reported by imprinting them on the signal or idler of an optical parametric oscillator (OPO) [1,2].

Here we report the first observation of creation and annihilation of polariton vortex-antivortex (V-AV) pairs by means of a short optical Gaussian pulse at a certain momentum k_{pb} . This observation sustains the superfluid character of polariton condensates and reveals their analogies with supercurrents in superconductors or persistent flow in condensates [1].

We have studied a $\lambda/2$ GaAs based microcavity with a Rabi splitting $\Omega_R=4.4$ meV. The sample is kept

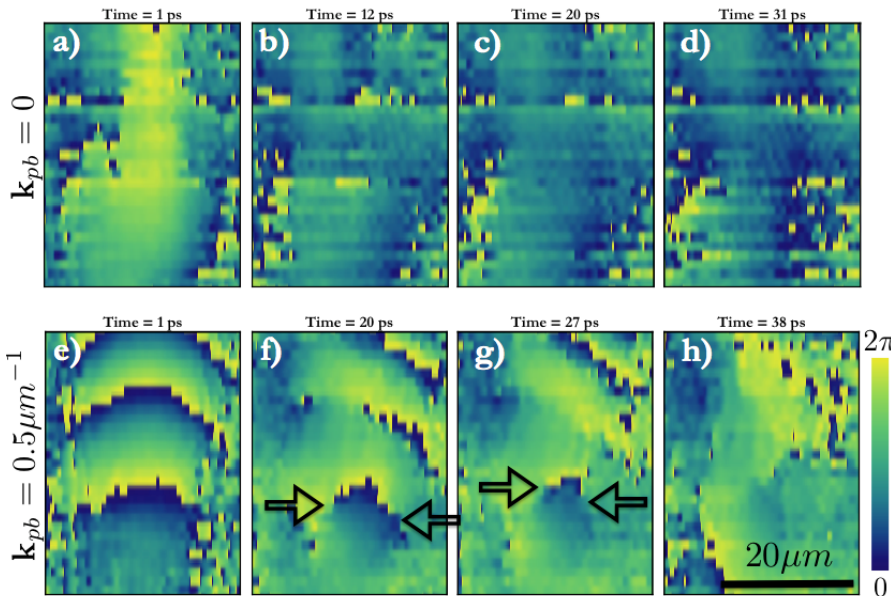


Fig 2. (a-d) Phase map dynamics for $k_{pb}=0$: no V-AV pairs appear, just an almost flat surface without apparent changes after the arrival of the probe is observed. (e-h) Phase map dynamics for $k_{pb}=0.5 \mu\text{m}^{-1}$. In snapshot e), $t=1$ ps after the probe has vanished, there is a slope in the phase, which starts the movement of polaritons and leads to the creation of a V-AV pair. (f-g) The V-AV pair is spontaneously created (see arrows) 4 ps after the probe disappearance and they come gradually closer to each other. h) The evolution of the V-AV pair leads to a self-annihilation after 30 ps. In all images the same spatial location of the sample is studied.

A 2 ps-long Gaussian probe, is injected in the OPO-signal to excite the polariton cloud in two different regimes $k_{pb}=0$ and $k_{pb}=0.5 \mu\text{m}^{-1}$ (see Fig. 2). The emission from the sample is analyzed in a Mach-Zender interferometer to perform phase-resolved imaging in time, with the help of a streak camera. This provides valuable information about V-AV formation and supercurrents dynamics in the OPO-signal. [3]

References

- [1] D. Sanvitto *et al.*, *Nature Phys.* **6**, 527 (2010)
- [2] D. Krizhanovskii *et al.*, *Phys. Rev. Lett.* **104**, 126402 (2010)
- [3] G. Tosi *et al.*, *Phys. Rev. Lett.* **104**, 126402 (2011)

* corresponding author : carlos.anton@uam.es

Double vortex dynamics in vertically coupled Permalloy dots

A. A. Awad^{1*}, A. Lara¹, M. García Hernández², V. Metlushko³, and F. G. Aliev¹

¹Dpto. Física Materia Condensada C-III, Universidad Autónoma de Madrid 28049 Madrid Spain,

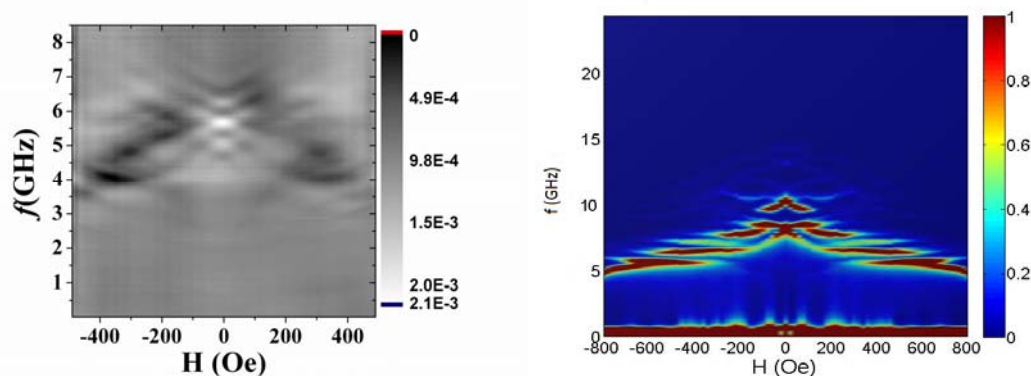
²Instituto de ciencias de Materiales ICMM,CISC, Cantoblanco, Madrid 28049, Spain;

³Dept. Electrical and Computer Engineering, University of Illinois Chicago IL, USA

The magnetic vortex state in circular dots has great potential for application in storage devices and spin torque oscillators. Recent studies predict qualitative change in spin wave and gyrotropic mode dynamics for two coupled circular magnetic dots [1,2]. Measurements of exchange coupled saturated dots also reveal substantial changes in the spin wave spectra [3,4].

Here we explore experimentally and by simulations, the static and dynamic response of the Py(25nm)/Cu(X)/Py(25nm) dots of 600 and 1000nm diameter and with spacer thickness X= 0.9 or 20nm. We investigate variation of both static and dynamic response between saturated and magnetic vortex states. The spin wave spectra of the uncoupled dots were published previously [5].

Analysis of magnetization reversal reveals that it corresponds to presence of magnetic vortices in each of the two dots Saturation (vortex annihilation) fields are larger for exchanged coupled dots with a 0.9nm thick Cu spacer. This observation shows that dipolar coupling, which is present in both types of the trilayer dots, is additionally strengthened by antiferromagnetic exchange coupling in the dots with ultrathin Cu spacer. In order to detect both low frequency gyrotropic and high frequency spin wave modes we used broadband FMR spectrometer. In agreement with theoretical predictions [1,2], the coupled Py dots in the vortex-vortex state reveal additional splitting of both gyrotropic and the lowest azimuthal modes. By sweeping the magnetic field reversibly without vortex annihilation, corresponding to the minor loop (i.e. without exceeding the minimum of two vortex annihilation fields), we study in detail the field dependence of the coupled azimuthal (optic and acoustic type) spin wave modes. Dynamic simulations using OOMMF (Fig. 1b), carried out for dipolar coupled vortices, are in qualitative agreement with experimental observations (Fig. 1a).



Fig(1). Magnetization dynamics experiment and simulation of double dots with dipolar coupling Py/Cu(20)/Py.

- [1] K.Yu. Guslienko, et al., Appl. Phys. Lett., **86**, 223112 (2005).
- [2] F. Montoncello, et al., J. Appl. Phys., **105**, 07E301 (2009).
- [3] M. Madami, et al., J. Appl. Phys. **105**, 07C115 (2009)
- [4] G. Gubbiotti, et al., Phys. Rev. **B73**, 144430 (2006).
- [5] F.G. Aliev, et al., Phys.Rev. **B79**, 174433 (2009).

Optical activation of BaMgF₄ ultra-transparent ferroelectric crystal

B. del Rosal^{1*}, P. Molina¹, M.O Ramírez¹, E.G Vllora², K. Shimamura² and L.E. Bausá¹

¹Dpto. Física de Materiales, Universidad Autónoma Madrid, 28049-Madrid, Spain

²National Institute for Materials Science, 1-1 Namiki, Tsukuba 305-0044, Japan

Ferroelectric materials frequently exhibit high values of their electro-optical, piezoelectric, pyroelectric and nonlinear coefficients, so that they are often used in advanced photonics and microelectronic devices applications. They have been successfully employed as high speed light modulators, parametric oscillators, and/or nonlinear frequency converters covering a wide range of the optical spectrum. Moreover, the extraordinary progress achieved, so far, in the micro-engineering of ferroelectric domains allows frequency conversion processes in a broad spectral range, sometimes only limited by the transparency range of the material. In addition, when conveniently doped with optical active ions they have also demonstrated laser action and intracavity self-frequency conversion processes, which substantially increase their multi-functionality in integrated photonics.

All these features have motivated us to explore the incorporation of Nd³⁺ and Yb³⁺ optically active ions in BaMgF₄, a ferroelectric crystal with an extraordinary transparency range which extends from the deep ultraviolet (~126 nm) to the mid-infrared (~13 μm) [1].

We present the optical properties of Nd³⁺:BaMgF₄ and Yb³⁺:BaMgF₄ crystals for their potential application as new self frequency-converted solid state lasers. High resolution site selective spectroscopy shows that Nd³⁺ (as well as Yb³⁺) ions are distributed at several well distinguished nonequivalent spectroscopic centers in the crystal lattice. Those centers are associated with different environments for Ba²⁺ cationic sites. We demonstrate that codoping with a monovalent cation (Na⁺) produces, in both cases, the annihilation of the minor centers to the benefit of the intensification of the optical emission lines associated with the major ones [2,3].

The effect of ferroelectric domain inversion on the spectroscopy of the optically active ions has also been studied. Furthermore, direct electron beam writing as been successfully used to produce ordered ferroelectric micro-domain patterns in Yb³⁺ doped BaMgF₄ with potential interest for optically active multifunctional photonic structures.

[1] E.G. Vllora, K. Sumiya, H. Ishibashi, and K. Shimamura, *Opt. Express* **17**, 12362 (2009).

[2] E.G. Vllora, P. Molina, S. Álvarez, J.V.García-Santizo, M.O Ramírez and K. Shimamura, and L.E. Bausa *J. Appl. Phys.* **107**, 033106 (2010).

[3] J.V. García Santizo, B. del Rosal, M.O Ramírez, L.E. Bausá, E.G. Vllora, P.Molina, V. Vasyliiev and K. Shimamura *J. of Appl. Phys.* **110**, 063102 (2011).

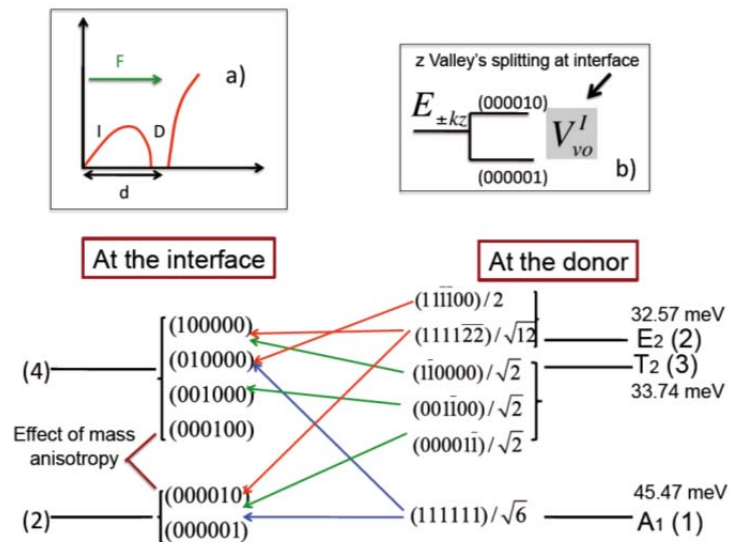
Electrical control of donor electrons in Si: valley composition and consequences for quantum computing.

A. Baena^{1*}, A. Saraiva², B. Koiller², and M.J. Calderón¹

1 Instituto de Ciencia de Materiales de Madrid, ICMM-CSIC
 2 Universidade Federal do Rio de Janeiro (Brazil).

Si-based quantum computing with donors is an interesting proposal that takes advantage of the technical development of the Si industry in the last decades. In this proposal, donor electrons are manipulated by electric fields applied by local gates. The conduction band of Si has six equivalent minima (valleys) leading to a degeneracy of the single electron ground state. The valley degeneracy is lifted at donors and (partially) at interfaces and is relevant for qubits definition, coherence and manipulation.

We model the problem of a single donor electron in Si close to a SiO₂ barrier under an applied electric field taking into account the full-valley description (see Figure). We are interested on the evolution of the valley composition of the electron ground state when it shuttles from the donor to the interface (and viceversa). The energy spectrum shows a set of (anti)crossings as a function of the electric field. The symmetry of the valley configurations of the states involved in the tunneling process, given by the (anti)crossing at lowest energy, depends on the distance d between donor and interface and on the valley splitting determined by the interface quality and the applied electric field. The consequences of the valley degeneracy on the qubit control are analyzed.



(a) Double well potential formed by the Coulombic donor potential plus the triangular interface/electric field potential. d is the distance between donor and interface. (Main panel) Symmetry of levels at the donor and at the interface. Every level is described by six coefficients corresponding to the six valleys of the conduction band of Si ($x, -x, y, -y, z, -z$). At the interface, the mass anisotropy breaks the valley degeneracy in a doublet and a quadruplet. The doublet degeneracy is further broken due to the valley orbit coupling, as shown in (b). At an isolated donor, the valley orbit coupling leaves a non-degenerate ground state with A_1 symmetry.

Magnetism and structure of amorphous Co-W alloyed nanoparticles

A. I. Figueroa^{1,2}, C. Magén^{2,3,4}, A. Ibarra³, L. Ruiz⁵, J. M. González-Calbet⁵, F. Petroff^{6,7},
C. Deranlot^{6,7}, S. Pascarelli⁸, P. Bencok⁸, N. B. Brookes⁸, F. Wilhelm⁸, A. Rogalev⁷,
F. Bartolomé^{1,2,*}, L. M. García^{1,2}, and J. Bartolomé^{1,2}

¹Instituto de Ciencia de Materiales de Aragón, CSIC - U. de Zaragoza. 50009 Zaragoza

²Departamento de Física de la Materia Condensada, Universidad de Zaragoza, C/ Pedro Cerbuna 12, 50009 - Zaragoza

³Instituto de Nanociencia de Aragón, Universidad de Zaragoza, 50018 - Zaragoza □

⁴Fundación ARAID, 50004-Zaragoza □

⁵Departamento de Química Inorgánica, Universidad Complutense de Madrid, E-28040 Madrid, Spain □

⁶Unité Mixte de Physique CNRS/Thales, F-91767 Palaiseau Cedex, France

⁷Université Paris-Sud, F-91405 Orsay Cedex, France

⁸European Synchrotron Radiation Facility (ESRF), F-38043 Grenoble, France

W-capped Co nanoparticles dispersed in an alumina matrix are studied by means of high-resolution transmission electron microscopy, extended x-ray absorption fine structure, SQUID-based magnetic measurements, ac magnetic susceptibility, and x-ray magnetic circular dichroism. Results show the formation of amorphous Co-W alloy nanoparticles, the magnetic properties of which are modified by the amount of W or Co present in the samples. The average Co magnetic moment depends on the number of W atoms surrounding it. Co-W particles show superparamagnetic behavior and are described as an array of noninteracting particles with random anisotropy axes and an average moment per particle proportional to the particle volume and to the average Co moment for each alloy composition. Values of the magnetic anisotropy constant of the particles are on the order of 10⁶ erg/cm³, higher than that of bulk Co. Evidence of short-range ordering within each amorphous particle is found that provides insight of the origin of their magnetic anisotropy.

Transferencia de energía en los molinos planetarios

J. S. Blázquez^{1*}, C.F. Conde¹, A. Conde¹

¹Dpto. Física de la Materia Condensada, Universidad de Sevilla, 1065, 41080, Sevilla, España

En este trabajo, mostraremos la ley que sigue la transferencia de energía en un molino planetario que consta de unos viales en los que se introduce el polvo del material a procesar junto a bolas de un material duro. Los viales rotan sobre un disco giratorio, con frecuencias ω y Ω , respectivamente. Las bolas atraparán el polvo al impactar entre ellas y con la pared del vial, transmitiendo así energía mecánica al material. El modelo empleado se simplifica al considerar: una sola bola, movimiento plano y bola en permanente contacto con la pared hasta que la fuerza normal aplicada por la pared, N , se anula. El análisis mecánico del problema [1] lleva a una expresión para N por unidad de masa de la bola, m : $N/m = \omega^2 r + \Omega^2 R \cos(\theta + \alpha)$ (parámetros definidos en figura 1a). Tanto el tiempo de despegue (para $N=0$) como el tiempo de vuelo de la bola tras éste (ver figura 1b) son inversamente proporcionales a Ω . Esto nos lleva a que el número de choques por ciclo, n , sea independiente de Ω y a que la frecuencia de golpeteo contra la pared sea $n\Omega$. Los choques de la bola contra la pared conllevan una cesión de parte de la energía cinética de la bola al polvo que queda atrapado en el choque. Esta energía cinética es proporcional a Ω^2 , con lo que finalmente tenemos que la potencia transferida es: $P = \frac{dE}{dt} = n\Omega E_{colisión} = A\Omega^3$, con A , una constante. En la figura 1c se muestra la temperatura externa del vial tras 30 min de molienda. Para este tiempo se alcanza una temperatura estable al igualarse el aporte de calor debido a los choques y la pérdida de calor a través de las paredes del vial: $\frac{dQ_{Total}}{dt} = A\Omega^3 - B\Delta T = 0$, resultando $\Delta T = k\Omega^3$.

Agradecimientos: MICINN y EU FEDER (MAT2010-20537) y PAI (P10-FQM-6462).

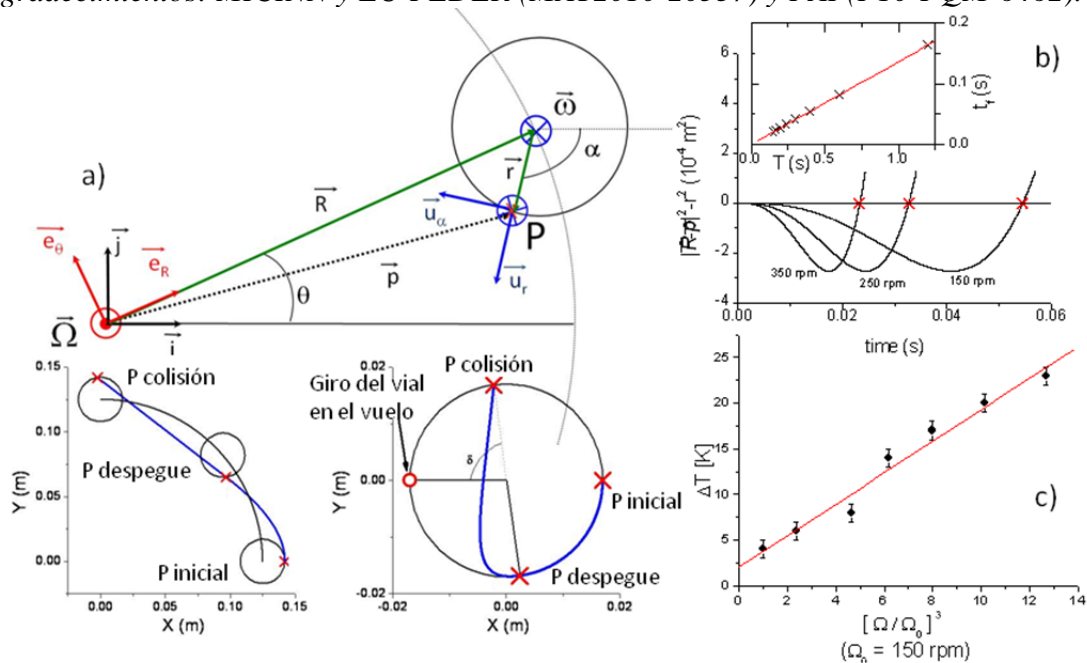


Figura 1: a) geometría del problema, b) cálculo del tiempo de vuelo y c) temperatura exterior del vial frente a Ω^3 .

[1] J.J. Ipus, J.S. Blázquez, V. Franco, M. Millán, A. Conde, D. Oleszak, T. Kulik, Intermetallics **16** (2008) 470-478.

Magnetic state and anisotropy in the Fe-based high T_c superconductors

M.J. Calderón*, B. Valenzuela, and E. Bascones

Instituto de Ciencia de Materiales de Madrid, ICMM-CSIC

Fe-based superconductors were discovered early 2008, with the highest superconducting critical temperatures (T_c) ever found after the record holding cuprates. The new superconductors develop the superconducting phase upon doping or applying pressure to a metallic anisotropic antiferromagnetic compound. The similarities with the cuprates (high T_c and antiferromagnetic parent phase) triggered a great deal of attention, which was further stimulated by the differences (undoped cuprates are Mott insulators, not metals) and by the perceived importance of the multiorbital character of the electronic carriers [1-4]. The properties of the magnetic phase itself are a subject of a strong debate due to the unexpected low magnetic moment, the different antiferromagnetic orderings encountered (columnar and bi-stripe), and a counter-intuitive resistivity anisotropy. Understanding these properties may be the key to unravel the origin of the superconductivity.

We will focus here on the anisotropy found in the columnar magnetic state in the xy -plane, with ferromagnetic order in one direction and antiferromagnetic in the other [5]. Contrary to expectations, the resistivity observed in the antiferromagnetic direction is lower than the resistivity in the ferromagnetic direction. The origin of this anisotropy is the subject of a strong debate in which orbital ordering and nematicity are usually invoked. The importance of the anisotropy resides in the consequences it may have for the pairing mechanism in the high T_c superconductors. We have shown [4] that the anisotropy is actually anticorrelated with orbital ordering and is instead related to the magnetic ordering through the topology and morphology of the Fermi surface.

- [1] M.J. Calderón, B. Valenzuela, and E. Bascones. Phys. Rev. B 80, 094531 (2009).
- [2] E. Bascones, M.J. Calderón, and B. Valenzuela. Phys. Rev. Lett. 104, 227201 (2010).
- [3] M.J. Calderón, G. León, B. Valenzuela, and E. Bascones, arXiv:1107.2279 (submitted).
- [4] B. Valenzuela, E. Bascones, and M.J. Calderón. Phys. Rev. Lett. 105, 207202 (2010).
- [5] J.-H. Chu et al, Science 329, 824 (2010) .

Processing and microstructure of spark plasma sintered 8Y-CSZ/5 vol% SWNT composites

E. Carrillo^{1*}, R. Poyato², A. Gallardo-López¹, A. Muñoz¹

¹Universidad de Sevilla, Departamento de Física de la Materia Condensada, Apdo. 1065- 41080 Sevilla, España

²Instituto de Ciencia de Materiales de Sevilla (CSIC-Univ. de Sevilla), Avda. Américo Vespucio 49, 41092 Sevilla, España

In this work, dense composites of cubic stabilized zirconia with 8 mol% yttria (8Y-CSZ) and 5 vol. % single walled carbon nanotubes (SWNTs) have been prepared by spark plasma sintering (SPS). This method has been proved as most efficient to sinter ceramic-carbon nanotube composites, since it achieves extremely high heating rates and allows full densification of the material at relatively low temperatures and pressures, and short sintering times, therefore minimizing degradation of the carbon nanotubes.

In order to obtain a homogeneous distribution of the SWNTs at the grain boundaries of the sintered composites, an acid treatment has been applied to the SWNTs previous to the ceramic powder mixture by colloidal processing and SPS sintering. This acid treatment is intended to separate and cut the SWNTs ropes in order to decrease their high tendency to agglomeration, and therefore avoid possible inhomogeneities in the composite microstructure. However, it has been shown to be very aggressive as it can destroy or damage a significant amount of nanotubes. For this reason, optimization of the treatment duration is crucial.

The microstructure of the sintered composites has been analyzed by high resolution scanning electron microscopy, showing a grain size in the submicrometer range in all of them. Also, the influence of the acid-treatment duration on the SWNT distribution in the ceramic matrix has been assessed on the sintered composites and Raman spectroscopy has been used to account for the integrity of the nanotubes. The sintering conditions have been proved to be adequate, and duration of the acid treatment should be in the range 6-8 hours. Composites with SWNT treated for 8 hours presented a most homogeneous microstructure, with the SWNTs entangling the ceramic grains, as can be seen in the SEM micrographs.

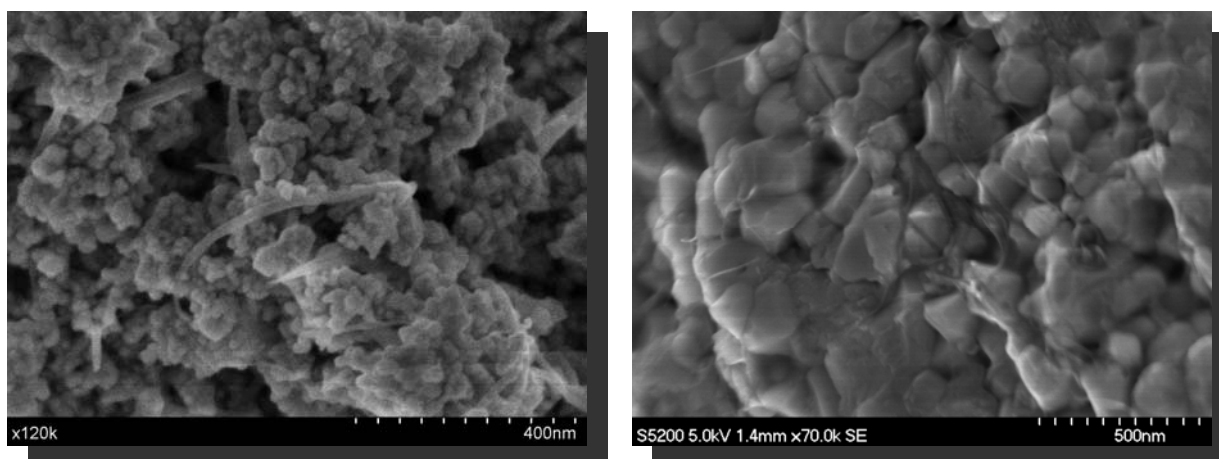


Fig. 1 SEM micrograph of 8Y-CSZ powder with 5% vol. SWNTs acid-treated for 8 hours before sintering (left), and after SPS sintering at 1100°C for 20 min. under 50 MPa applied pressure (right).

[1] R. Poyato, A.L. Vasiliev, N.P. Padture, H. Tanaka and T. Nishimura Nanotechnology **17** (2006) 1770-1777.

Flexible interference filters for UV radiation shielding applications

J.R. Castro Smirnov*, M. E. Calvo and H. Míguez

Instituto de Ciencia de Materiales de Sevilla, Consejo Superior de Investigaciones Científicas-Universidad de Sevilla, Américo Vespucio 49, 41092, Seville, Spain.

e-mail: jrcaastro@icmse.csic.es

Corresponding Author: José Raúl Castro Smirnov
Americo Vespucio 49, 41092 Seville, Spain

Abstract

Herein we present new flexible interference filters, based in hybrid nanostructures made with polymers and nanoparticles, for UV radiation protection. Flexible, self-standing multilayers were built by the alternating deposition of SiO_2 and Nb_2O_5 or ZrO_2 nanoparticulated suspensions in order to create a one dimensional photonic crystal (1DPC) of high dielectric contrast. Layers thicknesses were controlled through spin coater parameters to match the position of the Bragg reflection in the UV region of the spectrum. Furthermore, the large electronic bandgap of the metal oxides used in these structures (ZrO_2 , $E_g \cong 200\text{nm}$ and Nb_2O_5 , $E_g \cong 300\text{nm}$) allows for, covering the entire UVA, UVB and UVC ranges or a combination of them or for overlapping with the interference effects. Flexible films of Niobia and Zirconia 1DPCs were developed, infiltrating these porous structures with an elastomer (PDMS). After the polymerization of PDMS and a cooling treatment of the infiltrated multilayers, an easy lift-off process was carried out to obtain the self-supporting films. A complete optical characterization was performed, showing the evolution of the sample from pre-infiltration to flexible phase.

Anisotropic negative thermal expansion in $\text{Nd}_x\text{Co}_{1-x}$ thin films with perpendicular magnetic anisotropies

R. Cid^{1,2,*}, J. Díaz^{1,2}, L. M. Álvarez-Prado^{1,2}, R. Morales³, J. M. Alameda^{1,2}

¹ Universidad de Oviedo, C/ Calvo Sotelo s/n 33007 Oviedo, Spain

² Centro de Investigación en Nanomateriales y Nanotecnología – CINN (CSIC – Universidad de Oviedo – Principado de Asturias), Parque Tecnológico de Asturias, 33428 Llanera, Spain

³ Universidad del País Vasco/EHU, B° Sarriena s/n, 48940 Leioa, Bizkaia, Spain

* r.cid@cinn.es

Nd-Co amorphous thin films exhibit perpendicular magnetic anisotropy (PMA) even at real temperature [1], whose origin still remains a big challenge.

Single-ion anisotropy seems to be one of the main sources of this PMA [2] and an effective way to increase it in an amorphous alloy is by modulating its composition. Several studies have been carried out in compositionally modulated films (CMF) of Rare-earth–Transition-metals (RE-TM), showing that the PMA comes from the interface [2,3]. To go further in its comprehension, we've grown various alloys 100 nm thick of $\text{Nd}_x\text{Co}_{1-x}$ with different Nd concentration (around 17% and 21% of Nd atoms) by DC-magnetron sputtering. Two of them are CMFs obtained by alternated sputtering, while the other two are alloys prepared by co-sputtering. We maximize the amount of interface in the CMFs by growing Nd pseudomonolayers of only one atomic layer or less (around 2.9 Å) in both of them.

The anisotropy energies (K_N) in these samples as a function of temperature were estimated by VSM hysteresis loops and micromagnetic calculations. K_N ranged from 10^7 erg/cc at 10 K to 10^6 erg/cc at 300 K, not far from the crystalline values in RE-Co magnets. Higher differences were found in K_N between the CMFs than between the alloys, being K_N greater for the samples richer in Co.

The local microstructure in all the samples was studied by EXAFS, measuring Nd L3 and Co K spectra at normal and grazing incidence for 10 and 300 K. No EXAFS oscillations were detected in the Nd spectra, while Co EXAFS were well fitted using only Co scatters, suggesting a great disorder in the Nd environment.

An apparent negative thermal expansion (NTE) with λ as high as $-6 \cdot 10^{-3}$ is observed in the Co sublattice between 10 and 300 K. This NTE is anisotropic and behaves differently in alloys and CMFs: Co-Co at 10 K in alloys and CMFs expand preferentially in the normal to the film and the planar direction respectively. So that it happens at remanence, the NTE could be related with the reorientation of some oblate Nd ions whose easy axis rotate to point perpendicular to the film at 10 K. This is suggested by the narrowing of the stripe domains walls for decreasing temperature as pointed out by the evolution of remanent magnetization in the plane of the films.

[1] R. Cid, G. Rodríguez-Rodríguez, L.M. Álvarez-Prado, J. Díaz and J.M. Alameda, JMMM Vol. 316 (2007) e446-e449.

[2] Z. S. Shan, D. J. Sellmyer, S. S. Jaswal, Y.J. Wang and J. X. Shen, Phys. Rev. Lett. 63, 449 (1989).

[3] Y. Suzuki, H. Masuda, T. Shibata and N. Koshizuka, IEEE Trans. Magn. MAG-23, 3704 (1987).

Coherence of polariton condensates under OPO configuration

J. Cuadra^{1*}, R. Spano¹, C. Lingg¹, M.D. Martin¹, L. Viña¹, D. Sanvitto^{1†}, M. van der Poel² and J.M. Hvam²

¹Dept. Física Materiales, Universidad Autónoma de Madrid, Madrid 28049, Spain

²DTU Fotonik, Tech. Univ. Denmark, Ørstedes Plads 343 DK-2800 Kgs. Lyngby, Denmark

Coherence properties provide essential information about the nature of condensed phases and they are crucial to understand the analogies and differences between non-equilibrium, polariton condensates and either standard lasers or equilibrium condensates. Since the first report on exciton-polariton condensation in 2002 [1], and its unambiguous demonstration in 2006 [2], its coherence properties have been extensively investigated. Here, we study the first-order coherence properties of polariton condensates across the parametric threshold. We have found an extremely large coherence-length, just limited by the spot size, and a long coherence-time, lasting approximately six times more than those previously reported for similar cavities.

The experiments are performed under an optical parametric oscillator (OPO) configuration, on a λ GaAs microcavity with a 10 nm quantum well placed at the cavity field antinode and a Rabi splitting of ~ 4.2 meV. We use a ring-cavity, monomode laser to reduce fluctuations of polaritons populations and to limit the energy bandwidth of the excitation, and a relative large beam area ($\phi \sim 50 \mu\text{m}$) to obtain a true 2D condensate. Keeping the laser power constant, the threshold is obtained by tuning the excitation-laser wavelength to accomplish phase-matching conditions [3]. Its coherence properties are measured with a Mach-Zender interferometer, to obtain the first order correlation function $g^{(1)}$.

A finite correlation length is measured at an energy $\delta E = -0.19$ meV from the parametric threshold, as shown in Fig. 1(A, C). Once the threshold is reached the visibility extends across the entire condensate (Fig. 1(B, C)), as predicted by Carusotto and Ciuti [3]. A constant coherence is observed along $\sim 50 \mu\text{m}$, which is, to the best of our knowledge, the largest value reported up to now for 2D microcavities.

The coherence time is also enhanced significantly when reaching the parametric threshold. This is due to the fact that the system enters in the motional narrowing regime, where the rate of the fluctuations becomes larger than the linewidth of the macroscopic state. Our experimental results are well explained by the Kubo model for $g^{(1)}(\tau)$ [4] and evidence an increase in the coherence time of more than one order of magnitude, starting from $T_C \sim 100$ ps at $\delta E = -0.19$ meV (phase matching conditions not fulfilled) up to $T_C \sim 3$ ns at threshold. This is much longer than the highest value for the coherence time reported so far for GaAs microcavities, mostly limited by disorder, amounting to ~ 500 ps [5], for $10 \mu\text{m}$ condensates.

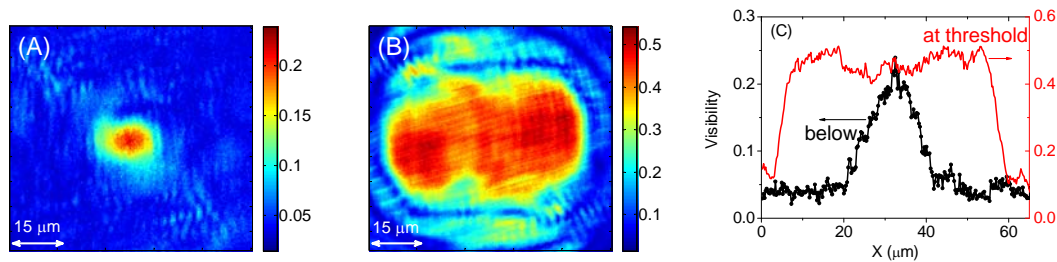


Fig.1: (A) Visibility map at $\delta E = -0.19$ meV from the signal state. (B) Visibility map at the OPO threshold. (C) Comparison of horizontal visibility profiles below (dots) and at (line) threshold: while (A) and (B) emissions (not shown) are comparable in size ($50 \mu\text{m}$) the visibility extension decreases strongly below threshold.

References

- [1] H. Deng *et al.*, *Science* **298**, 199 (2002).
- [2] J. Kasprzak *et al.*, *Nature* **44**, 409 (2006).
- [3] I. Carusotto and C. Ciuti, *Phys. Rev. B* **72**, 125335 (2005).
- [4] D.M. Whittaker and P.R. Eastham, *EuroPhys. Lett.* **87**, 27002(2008).
- [5] D.N. Krizhanovskii *et al.*, *Phys. Rev. Lett.* **97**, 097402 (2006).

* corresponding author: jorge.cuadra@uam.es

† present address: NNL/CNR. NanoScience Institut. Via Arnesano, 73100 Lecce. Italy

Probing the nuclear spin of a single donor in Silicon nanotransistors.

F. Delgado^{(1,2)*} and J. Fernandez-Rossier^(1,2)

(1) INL | International Iberian Nanotechnology Laboratory, Av. Mestre José Veiga, 4715-330 Braga, Portugal

(2) Departamento de Física Aplicada, Universidad de Alicante, San Vicente del Raspeig, 03690 Alicante, Spain

Abstract

Detection of a single nuclear spin constitutes an outstanding problem in different fields of physics such as quantum computing or magnetic imaging. Here we show that the energy levels of a single nuclear spin can be measured by means of a tunneling current [1]. As an example, we consider electronic transport through the single donor level of a Bismuth dopant in a Silicon nanotransistor, both in the sequential and in the cotunneling regimes, which has already been experimentally demonstrated [2,3]. In the sequential regime, the dI/dV curve yields the single electron spectral function, while in the cotunneling regime, it provides information about the electronic spin spectral function [4]. The hyperfine coupling to the nuclear spin results in a modification of the electronic spin spectral function which, in turn, could be probed by Inelastic Electron Tunneling Spectroscopy (IETS)[1,4-5], provided that the spectral resolution is high enough. We find that the hyperfine coupling opens new transport channels which can be resolved at experimentally accessible temperatures. Our simulations also evince that IETS yields information about the occupations of the nuclear spin states, paving the way towards transport-detected single nuclear spin resonance.

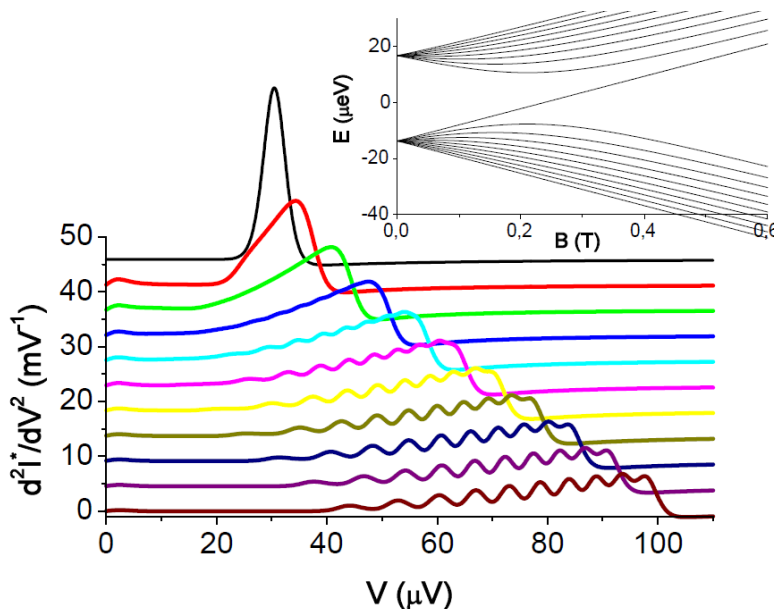
[1] F. Delgado and J. Fernández-Rossier, Phys. Rev. Lett. **107**, 076804 (2011).

[2] G. P. Lansbergen et al., Nano Letters **10**, 455 (2010).

[3] K. Y. Tan et al., et al., Nano Letters **10**, 11 (2010).

[4] J. Fernández-Rossier, Phys. Rev. Lett. **102**, 256802 (2009).

[5] F. Delgado, J.J. Palacios, and J. Fernández-Rossier, Phys. Rev. Lett. **104**, 026601 (2010)



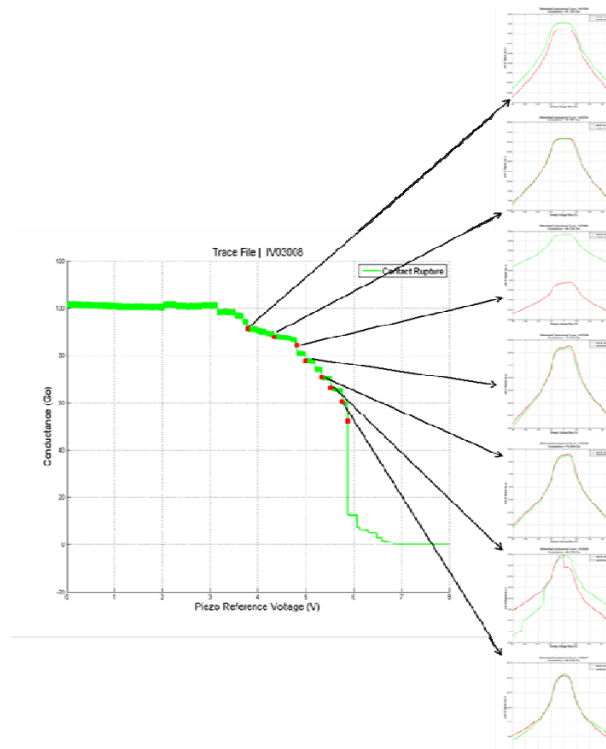
Energy spectrum of ^{209}Bi in Silicon as a function of applied field and the corresponding d^2I/dV^2 spectra at $T = 10\text{mK}$. Spectra for different fields from 0 (black line) to 0.6T (brown line) are shown shifted vertically for clarity.

Characterization of metallic nanocontact shape by electron-phonon interaction

T. Francisquez*, C. Sabater, G. Saenz-Arce, C. Untiedt

Departamento de Física Aplicada, Universidad de Alicante, Campus de San Vicente del Raspeig, E-03690 Alicante, Spain

Interpreting the conductance of a continually forming/breaking metallic nanocontact in terms of local atomic configurations near the narrowest section, nature of the valence electrons and presence of impurities has always been challenging due to intrinsic interplay between the atomic configurations, overlap of the conduction orbitals, and presence of impurities, all of which eventually allow for certain values of the conductance to be measured. Aside from expensive TEM or SEM in situ experiments, no other conclusive characterization technique exists that allows the determination of how the atomic configurations and local geometry of the nanocontact influence its conductance. In an attempt to shed increasing light on the nature of the atomic configurations and the local geometry of the contact, we performed point contact spectroscopy with a lock-in technique at several conductance values of a breaking gold nanocontact fabricated by STM indentation in a 4K and high vacuum system. By probing the electron-phonon interaction of the breaking nanocontact the local geometry was investigated. From the d^2I/dV^2 curves the position and magnitudes of the transverse acoustic (TA) peaks were extracted and their correlation to the local slope of the conductance trace and conductance value at which the spectroscopy curves were taken was investigated. An unclear tendency between the slope of the trace and the magnitude of the TA peaks is observed, whereas a clear shift of the TA peak position is observed as the conductance of the contact is decreased.



The effect of microstructure and interactions in the effective energy barrier distribution of granular Co-Zirconia films

M. García del Muro^{1,*}, Z. Konstantinović², X. Batlle¹ and A. Labarta¹

¹Dpt. de Física Fonamental i IN2UB, Universitat de Barcelona, Martí i Franquès 1, 08028-Barcelona, Spain

²ICMAB-CSIC, Campus UAB. E-08193 Bellaterra, Spain

Granular films, in which a distribution of ultrafine magnetic particles is embedded in a dielectric matrix are excellent materials to study basic properties, such as finite-size, interaction and surface effects. The present synthesis procedures allow preparing particles of controlled size and well dispersed in the solid matrix, and structural characterization methods provide the parameters such as shape, size distribution and interparticle distances that will be determinant of these effects. In particular, the dynamic magnetic behavior of the system will result from a complex interplay of these intrinsic properties and many-body effects associated with interparticle interactions

In this work, the time dependence of the thermoremanence was analyzed in terms of the $T\ln(t/\tau_0)$ scaling, since this method allows calculation of a time-independent effective distribution of energy barriers, which averages the contributions due to volume, shape and surface anisotropy and interparticle interactions. The evolution in the distribution with Co was interpreted taking into account particle size distributions obtained from transmission electron microscopy (TEM) and the weight of interactions extracted from first magnetization measurements such as low field magnetic susceptibility after zero field cooling (ZFC) and field cooling (FC). In summary: far from percolation, the effective energy barrier distribution presents a bimodal character. Although this behavior has been sometimes associated to the presence of interactions, in the present system can be justified from TEM results. Increasing the Co content, the maximum value and shape of the distribution slightly varies, as expected from the obtained microstructural parameters and low susceptibility measurements. However, in the medium range of Co concentration, a small increase in volume content results in a narrowing of the energy distribution, what could be associated with the presence of ferromagnetic correlations reflected in the FC curve. Finally, a last increase in Co content produces a large broadening of the energy barrier distribution, mainly due to the fact that close to the percolation threshold, particles start to coalesce, giving rise to larger non-spherical particles. Transport measurements confirm the evolution of particle sizes and the approximation to percolation.

Efecto de Haas van Alphen y Ceros de Spin en YBCO

David García-Aldea^{1,2*}, Sudip Chakravarty²

¹Departamento de Física Fundamental, UNED, Madrid Spain

²Department of Physics and Astronomy, UCLA, Los Angeles CA, USA

La naturaleza de la estructura de bandas de YBCO [1] continua siendo tema de debate en la literatura científica. En los últimos 3 años nuevos experimentos muestran oscilaciones cuánticas en la magnetización correspondientes al efecto de Haas van Alphen que proveen información cuantitativa muy valiosa acerca de como es la estructura de bandas de dicho superconductor en el régimen de dopaje inferior al dopaje óptimo. El origen de estas oscilaciones cuánticas se encuentra en el llenado de los niveles de Landau.

En este trabajo presentamos un modelo de estructura de bandas capaz de explicar cuantitativamente dichas oscilaciones así como las oscilaciones también medidas en la capacidad calorífica. En dicho modelo de bandas incluimos términos que dan cuenta del "hopping" en la dirección z entre los dos planos por celda unidad con los que cuenta el YBCO así como también entre celdas adyacentes. En los cálculos realizados se ha asumido que los candidatos para el parámetro de orden pueden ser los correspondientes a SDW (Spin Density Wave) o DDW (D Density Wave). La comparación con los resultados experimentales indica que el candidato más probable como parámetro de orden en este compuesto es DDW [2].

Otros experimentos más recientes muestran lo que se conoce como ceros de spin. Para ciertos valores del ángulo acimutal del campo magnético con respecto a los planos de cobre de YBCO se encuentra que independientemente de la intensidad del campo el valor de la magnetización es cero. Modificamos el modelo anterior para incluir que el parámetro de orden DDW puede ser singlete o triplete y comparamos también con los resultados para DDW. El modelo muestra que el estado singlete DDW es compatible con los ceros de spin medidos a los ángulos correspondientes mientras que el estado triplete haría aparecer dichos ceros de spin a ángulos mayores normalmente no accesibles en los experimentos realizados [3].

[1] Sudip Chakravarty. "Key issues in theories of high temperature superconductors," Rep. Prog. Phys. (Key Issues article), v.74, 2011, p. 022501.

[2] David Garcia-Aldea, Sudip Chakravarty. "Multiple quantum oscillation frequencies in $\text{YBa}_2\text{Cu}_3\text{O}_{6-d}$ and bilayer splitting," New Journal of Physics (Focus Issue on Fermiology in Cuprates), v.12, 2010, p. 105005.

[3] David Garcia-Aldea, Sudip Chakravarty. "Singlet versus triplet particle-hole condensates in quantum oscillations in cuprates," Phys. Rev. B, v.82, 2010, p. 184526.

Hysteresis and radiofrequency absorption behavior in epitaxial Au/Fe/Au/Fe/MgO films

M. Iglesias¹, E. Paz¹, F. J. Palomares¹, F. Cebollada², J. M. González³ and N. Sobolev⁴

¹Instituto de Ciencia de Materiales de Madrid (CSIC), Sor Juana Inés de la Cruz 3, E-28049 Madrid, Spain

²POEMMA, Departamento de Física Aplicada a las T.I., Universidad Politécnica de Madrid, E-28031 Madrid, Spain

³Unidad Asociada ICMM-CSIC/IMA-UCM, Sor Juana Inés de la Cruz 3, E-28049 Madrid, Spain

⁴Departamento de Física, Universidade de Aveiro, Aveiro, Portugal

We have prepared a series of epitaxial Au(9 nm)/Fe(X nm)/Au(9 nm)/Fe(1 nm)/MgO samples, with X = 3, 5 and 7 nm, by pulsed laser ablation deposition. The samples were structurally characterized by means of X-ray reflectivity and diffraction, which evidenced the occurrence of abrupt interfaces and the epitaxial character of the growth, respectively. As for the magnetic characterization, we have measured the angular (in-plane) dependence of i) the hysteretic processes by magneto-optic Kerr effect, and ii) the radio frequency absorption associated to the occurrence of ferromagnetic resonances (FMR). From our results we conclude that i) up to three different magnetization processes, showing different symmetries, can be identified on the loops measured along different in-plane field directions and ii) the angular dependence of the FMR evidenced the occurrence of absorption for fields applied along all the in-plane directions and four-fold symmetry. These results are analyzed in terms of the anisotropies and thicknesses of the Fe layers and of the interactions between them.

Confined magnetization state in thickness modulated amorphous NdCo₅ films with perpendicular anisotropy.

A.Hierro-Rodríguez^{1,2,*}, R.Cid^{1,2}, G.Rodríguez-Rodríguez^{1,2}, M.Vélez¹, J.I.Martín^{1,2},
L.M.Álvarez-Prado^{1,2} and J.M.Alameda^{1,2}

¹ Universidad de Oviedo, C/Calvo Sotelo s/n, 33007, Oviedo, Spain

² Centro de Investigación en Nanomateriales y Nanotecnología – CINN (CSIC – Universidad de Oviedo – Principado de Asturias), Parque Tecnológico de Asturias, 33428 Llanera, Spain
hierroaurelio@uniovi.es

Magnetic materials with out-of-plane magnetic anisotropy have a great interest nowadays due to their applications in high density magnetic storage medias. In the case of rare earth-transition metal alloys (RE-TM), these materials are also interesting from fundamental research point of view due to its complex magnetic behavior. One of the most interesting magnetic structures that appear in this kind of samples are the so called *Magnetic Stripe Domains*, whose existence is due to competition between magnetostatic energy, perpendicular and in plane anisotropies and exchange interaction [1, 2].

We have prepared amorphous NdCo₅ films with thickness modulations in grooved structures (Fig.1) by nanolithography techniques [3]. These kinds of structures allow us to study how the stripe domains configuration evolves as a function of magnetic film thickness and the grooves width, while the exchange interaction between the different regions of the nanostructure is present. Magnetic characterization has been made by magnetic force microscopy (MFM) technique with in-plane magnetic field application capability. Thus, MFM images sequences have been measured to analyze how the magnetization configuration evolves as a function of magnetic field.

The experiments show that there are two different magnetization behavior regimes related with the number of stripe domains that can exist in upper and lower regions. In the first regime large groove periods result in the existence of a great number of stripe domains both in the upper and lower regions of the nanostructured sample, and although both areas are exchange coupled, the magnetic behavior of each region seems to be decoupled, being even possible to obtain stripes configured in a perpendicular geometry (Fig.2a).

The other regime is observed when the structure's period is small compared with the stripe domain characteristic period, and then, the magnetization of the film becomes coupled again in the upper and lower regions (Fig.2b).

[1] L. M. Álvarez-Prado, G. T. Pérez, R. Morales, F. H. Salas, and J. M. Alameda, PRB, **56** (1997) 3306.

[2] R. Cid, G. Rodríguez-Rodríguez, L.M. Álvarez-Prado, J. Díaz and J.M. Alameda, JMMM, **316** (2007) E446.

[3] J.I Martín, J Nogués, Kai Liu, J.L Vicent and Ivan K Schuller, JMMM, **256**, 1-3 (2003) 449.

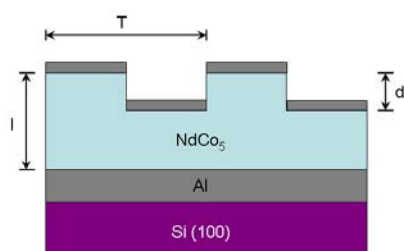


Fig.1 Sketch of a battlement - like structure in a NdCo₅ film.

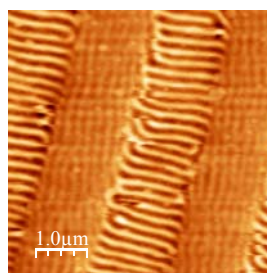


Fig.2a MFM image of battlement like structure with a period of 2 μ m showing the decoupled state.

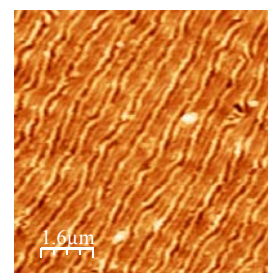


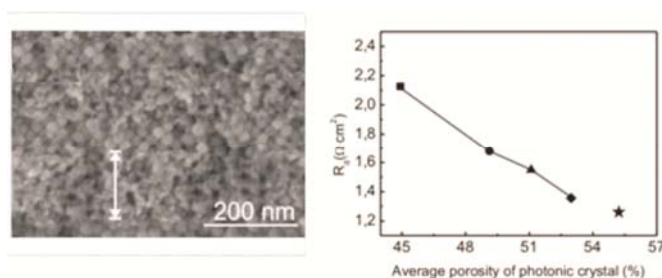
Fig.2b MFM image of structure with a period of 500nm showing the coupled state.

Photonic Crystals for Enhanced Light Harvesting in Dye Solar Cells.

Carmen López-López,* Silvia Colodrero, and Hernán Míguez.

Instituto de Ciencia de Materiales de Sevilla, Consejo Superior de Investigaciones Científicas-Universidad de Sevilla, Américo Vespucio 49, 41092, Sevilla, Spain.

Dye sensitized solar cells (DSSC) are photovoltaic devices based on the absorption of the sunlight by dye molecules to generate electricity. In order to improve the absorptance of the dye, the optical design of the cell can be modified by coupling nanoparticle 1D photonic crystal (1DPC)¹. This 1DPCs are built by the deposition of SiO₂ and TiO₂ nanoparticles.² This mirror is able to efficiently localize incident light within the sensitized electrode in a targeted wavelength range. Furthermore, its porous mesostructure allows the diffusion of the electrolyte through the layers. New methods for increasing the porosity and the pore size of these nanoparticle films in a controlled way, while preserving the optical quality, will be presented³. In this way, the mass transport through the crystal is improved, as confirmed by impedance measurements.



On right: FESEM image of a cross section of highly 1DPC showing the result of mixing a porogen with the nanoparticle suspensions and the annealing. On left: Diffusion resistance obtained at $j=0$ mA *versus* average porosity of the 1DPC prepared using different porogen:np-TiO₂ weight ratios, namely, 0 (square), 0.25 (circle), 0.5 (triangle), 0.75 (rhombus). Data for the multilayer prepared using both porogen:np-TiO₂ and porogen:np-SiO₂ weight ratios of 0.5 are also shown (star).

¹ S. Colodrero, A. Mihi, L. Häggman, M. Ocaña, G. Boschloo, A. Hagfeldt, H. Míguez, *Adv. Mater.*, 2009, **21**, 764.

² S. Colodrero, A. Mihi, J.A. Anta, M. Ocaña, H. Míguez, *J. Phys. Chem. C*, 2009, **113**, 1150.

³ C. López-López, S. Colodrero, S.R. Raga, H. Lindström, F. Fabregat-Santiago, J. Bisquert, and H. Míguez.

Molecular Prototypes for Spin-Based CNOT and SWAP Quantum Gates

F. Luis,^{1,*} A. Repollés,¹ M. J. Martínez-Pérez,¹ D. Aguilà,² O. Roubeau,¹ D. Zueco,¹ P. J. Alonso,¹ M. Evangelisti,¹ A. Camón,¹ J. Sesé,³ L. A. Barrios,² and G. Aromí²

¹ Instituto de Ciencia de Materiales de Aragón (ICMA), CSIC–Universidad de Zaragoza, and Departamento de Física de la Materia Condensada, Universidad de Zaragoza, E-50009 Zaragoza, Spain

² Departament de Química Inorgànica, Universitat de Barcelona, Diagonal 647, 08028, Barcelona, Spain

³ Instituto de Nanociencia de Aragón, Universidad de Zaragoza, and Departamento de Física de la Materia Condensada, Universidad de Zaragoza, E-50018 Zaragoza, Spain

In recent years, magnetic molecular clusters have been proposed as suitable materials for the realization of the quantum computer hardware [1]. Here, we show, via a combination of ac susceptibility, magnetization and heat capacity studies performed in the vicinity of the absolute zero, that molecular clusters containing two Tb³⁺ ions meet the ingredients required to implement a CNOT quantum gate [2]. The definition of control and target qubits is based on the strong magnetic anisotropy and the magnetic inequivalence of the two ions, which has been achieved by chemically engineering dissimilar coordination spheres. The magnetic asymmetry also provides a method to realize a SWAP gate in the same cluster. Electronic paramagnetic resonance experiments confirm that CNOT and SWAP transitions are not forbidden.

Although we have only considered Tb₂, for which the magnetic asymmetry can be easily determined on account of its large angular momentum, the same molecular structure can be realized with other lanthanide ions [3]. This flexibility enables a vast choice of quantum gate designs. These molecular clusters are stable in solution, which opens the possibility of depositing them onto devices able to manipulate its quantum spin state [4,5]. Chemically engineered molecular quantum gates can therefore open promising avenues for the realization of scalable quantum computing architectures.

[1] A. Ardavan, *et al*, Phys. Rev. Lett. **98**, 057201 (2007); S. Bertaina *et al*, Nature **453**, 203 (2008); G. Timco *et al*, Nature Nanotechnology **4**, 173 (2009).

[2] F. Luis, *et al*, Phys. Rev. Lett. **107**, 117203 (2011).

[3] D. Aguilà, *et al*, Inorg. Chem. (communication) **49**, 6784 (2010).

[4] A. Imamoglu, Phys. Rev. Lett. **102**, 083602 (2009).

[5] M. Urdampilleta, S. Klyatskaya, J-P. Cleuziou, M. Ruben, and W. Wernsdorfer, Nature Mater. **10**, 502 (2011).

Transport properties across $\text{LaAlO}_3/\text{La}_{2/3}\text{Sr}_{1/3}\text{MnO}_3$ (LAO/LSMO) interfaces

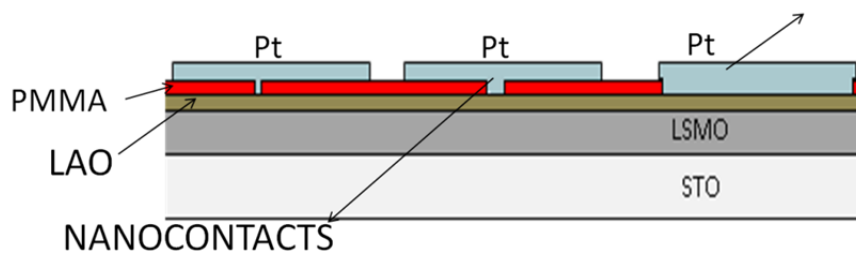
R. Galceran, L. Peña, A. Pomar, Z. Konstantinović, B. Bozzo Ll. Balcells,

F. Sandiumenge and B. Martínez

Institut de Ciència de Materials de Barcelona - CSIC,

Campus UAB. E- 08193 Bellaterra, Spain

The study of electronic transport properties of complex oxide interfaces is a subject of great interest; however it is a difficult issue from the experimental point of view. In order to have an easy access to the study of the magnetotransport properties across interfaces we have developed a nanostructured contact geometry enabling transport measurements by using the commercial PPMS (Physical Properties Measurement) system. $I(V)$ characteristic curves of the $\text{LaAlO}_3/\text{La}_{2/3}\text{Sr}_{1/3}\text{MnO}_3$ interface have been measured at room temperature by using a 2-point measurement station. The results are used to characterize the tunnel barrier using Simmons' model for intermediate voltage and to analyze the dependence on the nanocontact size in order to ensure a uniform current injection. Afterwards, $I(V)$ curves as a function of temperature and magnetic field can be safely measured by using the PPMS platform. The results are analyzed by using the Simmons' model for de intermediate voltage range.



Interfacial effects in manganite thin films with different capping layers

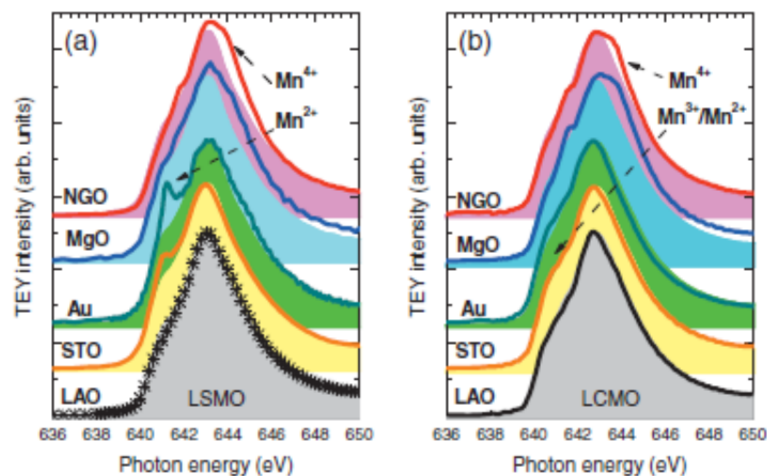
Z. Konstantinovic, R. Galceran, A. Pomar Ll. Balcells, F. Sandiumenge and B. Martínez

Instituto de Ciencia de Materiales de Barcelona-CSIC, Campus UAB. E-08193
Bellaterra, Spain

S. Valencia, D. Schmitz, A. Gaupp

Helmholtz-Zentrum-Berlin für Materialien und Energie, Albert-Einstein Str. 15 D-
12489 Berlin, Germany

Interfacial effects in sputtered manganite thin films with different capping layers (MgO, LAO, STO, NGO and Au) have been investigated. The interfaces have been chemically and magnetically characterized by means of local probes such as X-ray absorption spectroscopy (XAS) and X-ray magnetic circular (XMCD) and linear dichroism (XLD). Total electron yield detection at the Mn L-edge guarantees that the spectroscopic information originates from those regions closer to the film/capping interface. A complex phase separated scenario at the interface arises from the spectroscopic data. XAS shows departure of the Mn valence from bulk like values in case of STO and Au capping (Mn^{2+} presence) and in case of MgO and NGO (Mn^{4+} increase). XMCD shows concomitant depressed interface magnetization suggesting coexistence of ferromagnetic and non-magnetic phases. Finally XLD proves the presence of an antiferromagnetic (AFM) and orbital ordered (OO) phase.



Mn L3-edge absorption spectra for (a) LSMO and (b) LCMO films with different cappings obtained at $H = 0$ T after zero-field cooling

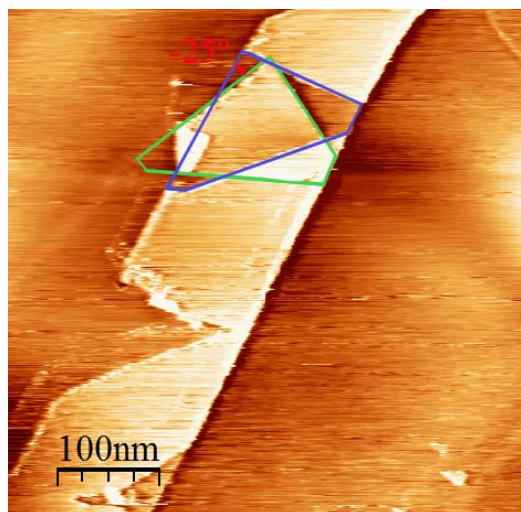
Fabrication and Characterization of folded Graphene on Graphite

D.C. Milan^{1*}, G. Saenz-Arce¹, M. Moaied², M.J. Caturla¹, J.J. Palacios² & C. Untiedt¹

¹Departamento de Física Aplicada, Universidad de Alicante, Campus de San Vicente del Raspeig, E-03690 Alicante, Spain

²Departamento de Física de la Materia Condensada, Universidad Autónoma de Madrid, Cantoblanco, 28049 Madrid, Spain

Nowadays, Graphene is one of the most studied carbon compounds due to their electronic properties. In this work, we demonstrate that Graphene, like a sheet of paper, folds under mechanical and electrostatic forces. Applying a electric pulse between Graphite surface and STM tip allow us to manipulate the upper layer of a Graphite surface forming voids, bend, move or decouple the upper Graphite layer or transfer part of the tip to the surface. Using *ab-initio* we can understand this effect by an electrostatic model calculations. MD simulations show a detachment effect of a temperature gradient or an uniaxial force on the upper layer of Graphite. Due to the different new discovered and studies physical-effects in Graphene edges, which can significantly influence the overall electronic and magnetic properties of graphene nanostructures, this results may be exploited as an *in-situ* method for Graphene exfoliation and different structures obtaining. Here we study Graphene flakes obtained with this Method. Once a sheet of Graphene is folded its structure and electronic properties are studied to determine its degree of coupling to the graphite substrate. Cross-sectional analysis of the fold shown reveals that it consists of a single sheet of graphite ($3,4\Delta^\circ$) folded. When the graphitic sheet bends, the bonding must lose some of its sp^2 character and gain some sp^3 character. So the ripples can be seen as sp^3 -like line defects in the sp^2 graphite sheets. The change from sp^2 to sp^3 -like character must always involve a pair of carbon atoms, as it is the π -bonding that is being disrupted. The sp^3 -like line defects should result in well defined edges in strongly curved graphite sheets.



Low temperature optical emission of wurtzite InAs nanowires

M. Möller^{1,*}, M. M. de Lima, Jr.¹, A. Cantarero¹, T. Chiamonte², M. A. Cotta², F. Iikawa²

¹Instituto de Ciencia de los Materiales, Universidad de Valencia, Catedrático José Beltrán 2, 46980 Paterna (Valencia), Spain

²Instituto de Física Gleb Wataghin, UNICAMP, CP 6165, 13083-970 Campinas, São Paulo, Brazil

Semiconductor nanowires have been widely investigated since they have an enormous potential for applications in advanced nanophotonic devices. In addition, it has been shown that III-V nanowires, such as InP, GaAs and InAs, can exhibit wurtzite crystal structure in contrast to the cubic zincblende phase of their bulk materials. The change in crystal structure alters the optical and electronic properties of the material, resulting in different fundamental physical parameters such as the band gap, exciton binding and phonon energies. In InAs, in particular, few data is available for the wurtzite phase. Theoretical works suggest a higher band gap energy than the one of the zincblende phase.^{1,2} Experimental data are very scarce, Trägårdh *et al.* have predicted an wurtzite band gap of 0.54 eV by extrapolating fitted photocurrent measurements on InAs_{1-x}P_x nanowires³ and Bao *et al.* observed a value of 0.52 eV in two-dimensional-like wurtzite structures.⁴

Here, we discuss photoluminescence measurements of wurtzite InAs nanowire samples grown by chemical beam epitaxy. Two samples containing nanowires with different stacking fault densities were studied. The InAs nanowires in both samples exhibit two main optical emission bands at low temperature. Excitation power dependent photoluminescence measurements show a blue-shift for the high energy band for increasing excitation powers, which is a typical behavior for type II interface heterostructure. Therefore, it was attributed to the quantum well emission formed by alternated wurtzite and zincblende sections in InAs along the wire, as has been observed for InP and GaAs nanowires.⁵ The type II band alignment for wurtzite and zincblende interface has been predicted theoretically.⁶ The low energy emission band is attributed to the donor-acceptor pair recombination in wurtzite InAs. Increasing the temperature both emission bands, as expected, decrease their intensity. The observed blue-shift of the high energy emission band indicates a higher band gap for the wurtzite structure of InAs compared to the one for the zincblende phase.

[1] Z. Zanolli, F. Fuchs, J. Furthmüller, U. von Barth, F. Bechstedt, Phys. Rev. B **75**, (2007) 245121.

[2] A. De, C. E. Pryor, Phys. Rev. B **81**, (2010) 155210.

[3] J. Trägårdh, A. I. Persson, J. B. Wagner, D. Hessmann, L. Samuelson, J. Appl. Phys. **101**, (2007) 123701.

[4] J. Bao, D. C. Bell, F. Capasso, N. Erdman, D. Wei, L. Fröberg, T. Martensson, L. Samuelson, Adv. Mater. **21**, (2009) 3654.

[5] T. B. Hoang, A. F. Moses, L. Ahtapodov, H. Zhou, D. L. Dheeraj, A. T. J. van Helvoort, B.-O. Fimland, H. Weman, Nano Lett. **10**, (2010) 2927.

[6] T. Akiyama, T. Yamashita, K. Nakamura, T. Ito, Nano Lett. **10**, (2010) 4614.

Incoherent interfaces and local lattice strains in solution-derived YBCO nanocomposites: a novel vortex pinning mechanism

A. Palau^{1,*}, Llordés¹, J. Gázquez^{1,2}, M. Coll¹, R. Vlad¹, A. Pomar¹, J. Arbiol¹, R. Guzmán¹, S. Ye¹, V. Rouco¹, F. Sandiumenge¹, S. Ricart¹, T. Puig¹, M. Varela², D. Chateigner³, G. Deutscher⁴, X. Obradors¹

¹Institut de Ciència de Materials de Barcelona, ICMA-B-CSIC, Campus de la UAB, 08193 Bellaterra, Catalonia, Spain

² Materials Science & Technology Division, Oak Ridge National Laboratory, Oak Ridge, Tennessee 37831, USA

³ Laboratoire de Cristallographie et Sciences des Matériaux, CRISMAT, ENSICAEN, IUT-Caen, Université de Caen Basse-Normandie, 6 boulevard Maréchal Juin, 14050 Caen Cedex 4, France.

⁴ School of Physics and Astronomy, Tel Aviv University, Tel Aviv 69978, Israel

Interfaces in oxides have become one of the most relevant issues to generate, enhance and control new physical phenomena. In many of the cases, interfaces have been promoted by growing nanocomposites where each phase is properly designed to undertake a specific role. Heteroepitaxial growth has therefore become the key process in controlling the strain of the designed *semicoherent* interfaces. Epitaxial growth of high temperature superconducting nanocomposites has emerged as a solution to control and enhance the vortex pinning landscape. In this work, we will demonstrate that a not so often used type of interface, *incoherent* interfaces, give rise to a new and highly effective vortex pinning mechanism in $\text{YBa}_2\text{Cu}_3\text{O}_7$ nanocomposites, where local lattice strains precludes Cooper pair formation inducing nanoscale regions effective for core pinning of vortices. For that purpose, solution-derived epitaxial nanocomposites with randomly oriented second phase nanoparticles (BaZrO_3 , Y_2O_3 , BaCeO_3 and Ba_2TaYO_6) were grown. This methodology has become an excellent low cost processing option generating a 3D ramified network of localized and highly strained nanoscale regions (mainly due to extra Cu-O chains and partial dislocations as evidenced by HRSTEM), responsible for huge quasi-isotropic pinning forces and a vanishing anisotropy of the critical currents.

Preferencia: Oral

Vortex lattice motion induced by alternating forces in superconducting magnetic hybrid nanostructures

D. Perez de Lara^{1,2}, F. Galvez², M. A. Garcia³, E. M. Gonzalez², and J. L. Vicent^{1,2}

¹IMDEA-Nanociencia, Cantoblanco, 28049 Madrid, Spain

²Departamento Física Materiales, Facultad Ciencias Físicas, Universidad Complutense, 28040 Madrid (Spain)

³Instituto de Cerámica y Vidrio CSIC, Cantoblanco, 28049 Madrid (Spain)

We have fabricated hybrid nanostructures with Nb film on top of an array of Ni nanotriangles. In these structures, non-zero DC and AC voltages (VDC, VAC) are generated by alternating currents injected in the hybrid device. The VDC and VAC behaviors give us an overall picture of the vortex dynamics and the rectification effects in these superconducting devices.

[1] C. S. Lee, B. Janko, I. Derényi, and A. L. Barabasi, *Nature (London)* **400**, 337 (1999).

C. S. Lee, B. Janko, I. Derényi, and A. L. Barabasi, *Nature (London)* **400**, 337 (1999).

[2] J. Mannhart, *Supercond. Sci. Technol.* **9**, 49 (1996).

[3] J. E. Villegas, S. Savel'ev, F. Nori, E. M. González, J. V. Anguita, R. Garcia, and J. L. Vicent, *Science* **302**, 1188 (2003).

[4] P. Hänggi and F. Marchesoni, *Rev. Mod. Phys.* **81**, 387 (2009)

Magnetite nanoparticles with bulk like behaviour

N. Pérez^{1,*}, F. Bartolomé², L.M. García², J. Bartolomé², A.G. Roca³, M. P. Morales³, C.J. Serna³, F. López-Calahorra⁴, A. Labarta¹, X. Batlle¹

¹Dep. Física Fonamental and Institut de Nanociència i Nanotecnologia (IN2UB), Universitat de Barcelona, Martí i Franquès 1, 08028 Barcelona, Spain

²Instituto de Ciencia de Materiales de Aragón (ICMA)-CSIC and Dep. Física Materia Condensada, Universidad de Zaragoza, 50009 Zaragoza, Spain

³Instituto de Ciencia de Materiales de Madrid (ICMM)-CSIC, 28049 Madrid, Spain

⁴Departament de Química Orgànica and Institut de Nanociència i Nanotecnologia (IN2UB), Universitat de Barcelona, Martí i Franquès 1, 08028 Barcelona, Spain

Key questions in nanostructured magnetic materials are how the nanostructure modifies their magnetic and electronic properties, giving rise to new phenomena taking place at the nanoscale as a consequence of the interplay of quantum, finite-size, surface, and interfacial effects, and how one can take advantage of those new properties to improve the applications.

Here we address the origin of the enhanced magnetic and electronic properties presented by magnetite nanoparticles synthesized by high temperature decomposition of organometallic iron precursors with oleic or decanoic acid as surfactant.

Transmission electron microscopy, x-ray absorption spectroscopy, x-ray magnetic circular dichroism, and magnetization measurements show that nanoparticles synthesized by thermal decomposition display high crystal quality and bulk-like magnetic and electronic properties, while nanoparticles synthesized by coprecipitation show much poorer crystallinity and particle-like phenomenology, including reduced magnetization, high closure fields, and shifted hysteresis loops [1,2]. Additionally, Monte Carlo simulations show that intrinsic finite-size and surface effects are relevant only for sizes below about 5 nm. All in all, these results suggest the key role of the crystal quality in the magnetic and electronic properties of ferromagnetic nanoparticles and, in particular, the fact that, in many cases, the magnetic disorder phenomena observed in single-phase particles larger than a few nanometers in diameter should not be considered as an intrinsic effect associated with the finite size [2].

The process of formation of high quality magnetite nanoparticles by thermal decomposition was investigated by liquid chromatography and mass spectroscopy, showing that the dissociation into radicals of the bonds between the iron atoms and the fatty acid provides the reduction of the Fe(III) cations and the oxygen atoms required for the formation of the mixed-valence inverse spinel magnetite structure [3]. Depending on the starting precursor the morphology of the particles is altered and the magnetic properties can be optimized.

Finally, high quality magnetite nanoparticles are suitable for biomedical applications after stabilization in physiological conditions, allowing enhanced resolution in applications such as magnetic resonance imaging or biodistribution [4]. The study of the distribution and clearance of magnetite nanoparticles in mice organs by magnetization measurements shall be presented.

[1] N. Pérez, F. Bartolomé, L. M. García, J. Bartolomé, M. P. Morales, C. J. Serna, A. Labarta and X. Batlle, *Appl. Phys.Lett.* **94** (2009) 093108.

[2] X. Batlle, et al., *J. Appl. Phys.* **109** (2011) 07B524.

[3] N. Pérez, F. López-Calahorra, A. Labarta and X. Batlle. *Phys. Chem. Chem. Phys.* **13** (2011) 19485.

[4] R. Mejías, et al., *Nanomedicine* **5** (2010) 397.

Optimization of the thermoelectric figure of merit through the fabrication of compositesB. Rivas-Murias^{1,2,*}, F. Rivadulla^{1,2}¹Centro de Investigación en Química Biológica y Materiales Moleculares (CIQUS)²Departamento de Química-Física, Universidad de Santiago de Compostela, 15782 Santiago de Compostela, España

One of the most important challenges for today's society is to develop green and sustainable energy sources, at the time that the efficiency of the energy use is substantially increased for the existing technologies.

Efficient thermoelectric modules pose an interesting and promising solution for high-temperature energy harvesting and cooling. The TE conversion efficiency is characterized by the figure of merit $ZT=S^2T/\rho\kappa$, where ρ , S and κ are the electrical resistivity, the Seebeck coefficient, and the thermal conductivity, respectively [1,2]. Consequently an efficient thermoelectric material should present low ρ , high S and low κ , difficult to achieve due to the interrelationships among these parameters.

The layered cobalt oxides, such as $\text{Ca}_3\text{Co}_4\text{O}_9$ and Na_xCoO_2 [3,4], seem to be interesting candidates due to their chemical stability and absence of hazardous elements. However, their large thermal conductivities (common to most oxide materials) limited their practical application.

In the present work, we have focused on the synthesis and characterization of the composites formed by $\text{Ca}_3\text{Co}_4\text{O}_9$, carbon black and poly(vinyl acetate). Nanoparticles of $\text{Ca}_3\text{Co}_4\text{O}_9$ were synthesized by sol-gel method at 750°C. The mechanical and electrical properties of carbon black make it a good candidate to combine with dense oxide thermoelectrics, as it helps maintaining a large electronic conductivity. PVA was used as binder to obtain resistant pellets without further thermal treatment (room temperature processing). Intergrain boundary scattering reduce the thermal conductivity in these composites, increasing ZT .

We will present the results of ZT in these composites as a function of composition and will discuss future strategies for further optimization of the thermoelectric performance.

[1] B. Sales, *Current Opinion in Solid State and Materials Science* **2** (1997) 284.

[2] T. M. Tritt, M.A. Subramanian, *MRS Bulletin* **31** (2006) 188.

[3] M. Mikami, N. Ando, R. Funahashi, *Solid State Chem.* **178** (2005) 2186.

[4] I. Terasaki, Y. Sasago, K. Uchinokura, *Phys. Rev. B* **56** (1997) R12685.

Effects of agglomeration on nanoparticles properties studied by confocal Raman microscopy

J.J. Romero^{1,*}, I. Lorite¹, A. del Campo, J.F. Fernandez¹

¹Instituto de Cerámica y Vidrio, CSIC, C/Kelsen 5, 28049-Madrid, Spain

The interest on the properties of nanoparticles is widely known and do not need to be further mentioned. Most of the works up to now have dealt with the fabrication of nanoparticles and the study of the relation between their size and their properties. It is widely accepted that the properties of nanoparticles depend dramatically on their size and the nature of their surface (due to the large surface/volume they present). Nevertheless, few works have studied the possible effects of the environment on their properties, and more particularly, the effects of their agglomeration.

Although it is widely known that nanoparticles present a high tendency to agglomerate and different strategies have been followed to avoid this agglomeration, no techniques have been described that can be used to control the agglomeration state of the nanoparticles. In this work, we present a method to control the agglomeration state of nanoparticles and study their Raman properties as a function of the agglomeration state.

The Raman spectra of isolated nanoparticles and agglomerates were obtained with a Confocal Raman Microscope (CRM). The spatial resolution of such system is about 300 nm, being then not enough for a univocal characterization of nanoparticles. To overcome the resolution of CRM, a new technique called INARS (Isolated Nanoparticles Raman Spectroscopy) [2] has been followed. In this technique, a Atomic Force Microscope (AFM) is used in collaboration with the CRM to get results from isolated nanoparticles as well as from clusters of well defined size.

The results clearly show that the agglomeration state modifies the Raman spectrum of the nanoparticles. In the particular case of Co_3O_4 nanoparticles (25 nm diameter), the main Raman mode (A_{1g}) of isolated nanoparticles appears at 691 cm^{-1} , in surprisingly good accordance with the value found on microcrystals, while for agglomerates of about 200 nanoparticles a red shift of this mode of up about 30 cm^{-1} have been observed. These results clearly indicate that care must be taken when studying the Raman properties of nanoparticles.

[1] I. Lorite, A. del Campo, J.J. Romero, J.F. Fernández, Journal of Raman Spectroscopy (in press)

Vortex dynamics in YBCO films with engineered antidots and ferromagnetic nanostructures

V. Rouco^{1*}, A. Palau¹, C. Monton¹, T. Puig¹, X. Obradors¹, G. Via², C. Navau², N. del Valle²,
A. Sánchez², R. Córdova³, J.M. de Teresa³

¹Institut de Ciència de Materials de Barcelona (ICMAB-CSIC), Bellaterra, Barcelona, Spain

²Universitat Autònoma de Barcelona (UAB), Bellaterra, Barcelona, Spain

³Instituto de Nanociencia de Aragón, Universidad de Zaragoza, E-50009 Zaragoza, Spain

Understanding vortex pinning mechanisms and the interaction between vortices and defects is still one of the major goals to enhance efficiencies of superconductors. We have used the Focused Ion Beam (FIB) technique to create artificial pinning sites in YBCO thin films grown by chemical methods. Model systems with antidots have been generated by using the FIB as a high resolution milling technique. Moreover, with this aim to study interactions in hybrid superconductor-ferromagnetic systems we have filled the antidots with cobalt rods by focused electron beam induced deposition.

In-field transport critical current measurements have been performed in a wide temperature (T) and magnetic field ($\mu_0 H$) ranges in order to study vortex dynamics in these novel systems. As far as YBCO thin films with ferromagnetic rods, we demonstrate a clear interaction between the magnetic field generated by the cobalt nano-rods and the superconducting matrix. Theoretical calculations have been performed in order to analyze the local magnetic field in the YBCO matrix, modified by the trapped magnetic field in the superconductor and the magnetization of the ferromagnetic nano-rods.

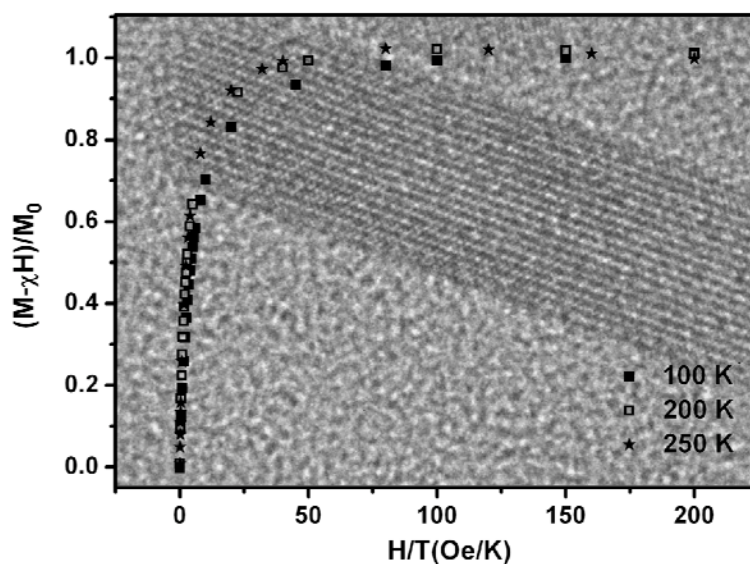
Preferencia: Poster

Goethite (α -FeOOH) Nanorods as Suitable Antiferromagnetic Substrates

Verónica Salgueiriño,* Rosalía Mariño-Fernández

¹Universidade de Vigo, Department of Applied Physics, 36310 Vigo, Spain

We propose goethite nanorods as suitable antiferromagnetic substrates. The great advantage of using these inorganic nanostructures as building blocks comes from the fact that permits the design and fabrication of colloidal and supracolloidal assemblies knowing first their magnetic characteristics. As a proof of concept we have developed mix multifunctional systems, driving on the surface of these AFM substrates, cobalt ferrite nanoparticles (the study of bimagnetic systems opens new degrees of freedom to tailor the overall properties and offers the Meiklejohn-Bean paradigm but inverted), a silica shell (protection purposes but also as tailored spacer that permits to control magnetic interactions) and metallic gold clusters (seeds that can favor the acquisition of optical or catalytic properties).[1]



[1] R. Mariño-Fernández, S. H. Matsunaga, N. Fontaiña-Troitiño, M. P. Morales, J. Rivas, V. Salgueiriño, *J. Phys. Chem. C* **115**, (2011) 13991.

Combined surface plasmon resonance and X-ray absorption spectroscopyA. Serrano^{1,*}, O. Rodríguez de la Fuente², G. R. Castro³ and M .A. García^{1,4}¹Institute for Ceramic and Glass, CSIC, Madrid, Spain²Dpt.Materiales Physics, Universidad Complutense, Madrid, Spain³Spline Spanish CGR beamline at ESRF, ICMM-CSIC, Grenoble, France⁴IMDEA Nanociencia, Madrid, Spain

We present a system for the excitation and measurement of surface plasmons in metallic films based on the Kretschmann-Raether configuration that can be installed in a synchrotron beamline. The device was mounted and tested in a hard X-ray Absorption beamline, BM25 Spline at ESRF. With this device it is possible to carry on experiments combining surface plasmon and X-ray absorption spectroscopies. The surface plasmons can be used to monitor *in situ* changes induced by the X-rays in the metallic films or the dielectric overlayer. Similarly, the changes in the electronic configuration of the material when surface plasmons are excited can be measured by X-ray absorption spectroscopy. The resolution of the system allows observing changes in the signals of the order of 10^{-3} to 10^{-5} depending on the particular experiment and used configuration. The system is available for experiments at the beamline.

Manganese phthalocyanine on metallic surfaces: From Kondo effect to magnetoresistance.

M. Soriano^{1,*}, J.J. Palacios¹

¹Universidad Autonoma de Madrid. Departamento de Fisica de la Materia Condensada. Campus de Canto Blanco. Madrid. Spain.

Manganese Phthalocyanine (MnPc) is an organic molecule hosting a Mn atom with three unpaired electrons. After deposition on surfaces, phenomena such as underscreened Kondo effect or magnetoresistance can emerge when probed with a STM tip, depending on the nature of the surface and the tip. Motivated by recent experimental and theoretical works [1-4], we try to understand the origin of the Kondo resonance observed in bare MnPc molecules and in CO decorated ones adsorbed on different metal surfaces. Also we try to understand the interaction between the MnPc on a highly magnetized manganese surface, centering our attention onto the tunneling magnetoresistance phenomena and its dependence on the different adsorption sites. With this aim we have performed computational studies based on Density Functional Theory (DFT) using our ANT code [5]. The Landauer formalism has been used to compute transport properties and we have computed the hybridization function to predict the Kondo Resonance.

[1] N. Tsukahara; et. al. Phys. Rev. Lett. 102, 167203 (2008)

[2] C. Iacovita et.al. Phys. Rev. Lett. 101, 116602 (2008)

[3] K. J. Franke et. al. Science 332, 940 (2011)

[4] M. Karolak et. al. Phys. Rev. Lett. 107, 146604 (2011)

[5] J. J. Palacios et.al. ANT. Ab-Initio Quantum Transport. <http://alacant.dfa.ua.es>.

Soft plasma processing of organic nanowires: a route for the fabrication of 1D organic heterostructures and the template synthesis of inorganic 1D nanostructures

M. Alcaire,^{1*} J. R. Sanchez-Valencia,¹ F. J. Aparicio,¹ Z. Saghi,^{2,3} J. C. Gonzalez-Gonzalez,¹ A. Barranco,¹ Y. Oulad-Zian,¹ A. R. Gonzalez-Elipe,¹ P. Midgley,² J. P. Espinos,¹ P. Groening⁴ and A. Borras¹

¹Instituto de Ciencia de Materiales de Sevilla (ICMS, CSIC-US), Nanotechnology on Surfaces Lab., C/ Américo Vespucio 49, 41092, Sevilla, Spain.

Switzerland

²Department of Materials Science and Metallurgy, University of Cambridge, Pembroke Street, CB2 3QZ. Cambridge, UK.

³BIONAND (Andalusian Centre for Nanomedicine and Biotechnology), Parque Tecnológico de Andalucía, c/ Severo Ochoa, 35, 29590 Campanillas, Málaga, Spain

⁴EMPA, Swiss Federal Laboratories for Materials Science and Research, Nanotech@surfaces Lab., Uberlandstrasse 129, 8600, Dubendorf, Switzerland

The emerging field of organic nanowires (ONWs) is settling down thanks to the effort carried out during the last years in both the fabrication and the study of their properties. The outstanding performance of 1D organic nanostructures based on small molecules has been proved in photonics, photovoltaic, photocatalysis, microelectronic and nanosensing applications. Parallel with the inorganic counterpart, the fabrication of heterostructured organic nanowires is increasingly gaining interest because of their use in the aforementioned fields of applications as well as in the study of model systems for 1D n-p heterojunctions. Within this framework in this communication we report about an unprecedented route for the synthesis of heterostructured organic nanowires which consist of the combination of two well established vacuum processes, namely the synthesis of single crystal supported organic nanowires by physical vapour deposition and oxygen plasma etching. The possibilities of this methodology are illustrated with the fabrication of two different types of organic nanostructures: heterostructured hierarchical NWs and metal-organic hybrid NWs. Moreover, we go a step forward in the use of plasmas by describing the first results of an original template method for the synthesis of inorganic 1D nanostructures by processing organic nanowires. We also demonstrate that by controlling the intensity of the plasma treatment, the method can be used to fabricate hierarchical 1D organic heterostructures formed by two or more interconnected ONWs.¹

[1] M. Alcaire, J. R. Sanchez-Valencia, F. J. Aparicio, Z. Saghi, J. C. Gonzalez-Gonzalez, A. Barranco, Y. Oulad-Zian, A. R. Gonzalez-Elipe, P. Midgley, J. P. Espinos, P. Groening and A. Borras *Nanoscale* 2011, 3, 4554-4559.

Nanostructure of thin films grown by deposition of isotropically distributed gaseous particles at low temperatures

R. Álvarez^{1*}, P. Romero-Gomez¹, J. Gil-Rostra¹, J. Cotrino^{1,2}, F. Yubero¹, A. Palmero¹, A. R. Gonzalez-Elipe¹

¹Instituto de Ciencia de Materiales de Sevilla, c/ Américo Vespucio 49, 41092 Seville, Spain

² Universidad de Sevilla, Departamento de Física Atómica, Molecular y Nuclear, Av. Reina Mercedes s/n, 41012 Seville, Spain

Preference: Poster presentation.

Abstract.-

One of the most important factors that determine the formation of a given film microstructure is the angular distribution of the deposition flux. This distribution function strongly affects the surface shadowing mechanism, by which taller surface features inhibit the deposition of other particles under their shadow. In this work we theoretically and experimentally characterize the growth of amorphous thin films under the following constrains: i) the film temperature is low enough to inhibit surface diffusion and crystallization mechanisms, ii) the interaction plasma/film surface is weak during growth, and iii) the deposition flux follows an isotropic velocity distribution function in the gaseous phase before being deposited. From an experimental point of view, we employed two different deposition techniques: Inverse magnetron sputtering (i-MS) deposition, which corresponds to a typical magnetron sputtering setup, but placing the film at the backside of the substrate holder (i.e., not facing the cathode), and plasma enhanced chemical vapor deposition (PECVD), by which we used volatile precursors in a downstream configuration. We have studied different amorphous TiO₂ and SiO₂ thin films deposited under the abovementioned conditions, finding that all of them share common microstructural features: all of them possess a coalescent column-like vertical microstructure, whose features are discussed through the experimental characterization of the films and the assistance of a Monte Carlo model of the growth.

* Corresponding author:

Dr. Rafael Alvarez Molina

Email: rafael.alvarez@icmse.csic.es

High frequency matching effects of superconducting Pb films with magnetic vortex periodic pinning

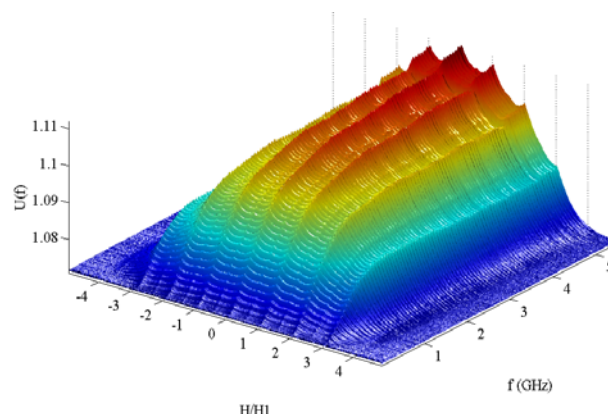
A.A. Awad^{1*}, A. Lara¹, A.V. Silhanek², G.W. Ataklti², V.V. Moshchalkov², F.G. Aliev¹

¹Departamento de Física de la Materia Condensada C-III, Universidad Autónoma de Madrid 28049 Madrid Spain.

²INPAC-Institute for Nanoscale Physics and Chemistry, Katholieke Universiteit Leuven, Celestijnenlaan 200D, B-3001 Leuven, Belgium

Magnetic and superconducting vortices could interact in hybrid superconductor / ferromagnet structures [1-3]. Theoretically [1] it had been predicted that pinning of the vortex line by the nanodisk being predominantly from the interaction between the vortex line and the changes in the nanodisk magnetization induced the displacement of the magnetic vortex. Experimental reports on the influence of magnetic vortex state [2] and the pinning enhancement [3] on Superconducting films. Later, Shapoval *et al.* [4] have found that the magnetic vortex core for Nb films over Py dots introduced only weak additional pinning.

Here we report on broadband microwave response (300 kHz to 8.5GHz) in the 90 and 50 nm thick superconducting Pb films deposited on top of array of 1000 nm diameter and 35nm thick circular Py dots in the vortex ground state and arranges in square lattice with period of 2000 nm. At temperatures close to about $0.95T_c$ we find periodic variation of the microwave permeability as a function of external magnetic field. We clearly detect few interger (H_n) and rational ($H_{k/m}$) matching fields which are in accordance with recent measurements of microwave complex reflection on 50nm thick Pb film with periodic array of microholes inside *rf* coil [5]. In addition, we found that the variation of the relative amplitude of integer and rational pinning anomalies with frequency and microwave power indicates a transition from microwave induced vortex depinning at lowest *rf* powers (which increases the magnitude of the permeability anomalies) to *rf* induced heating which substantially decreases the matching anomalies in permeability. Finally, we investigate the influence of the vortex core alignment (cores up or down) on the asymmetry of the microwave response vs. magnetic field.



Fig(1). Frequency-field dependence of the mictowave response close to T_c .

- [1] G. Carniero, Physica **C460–462** 1186 (2007).
- [2] J. Villegas, *et al.*, Phys. Rev. Lett., **99**, 227001 (2007).
- [3] A. Hoffmann, *et al.*, Phys. Rev. **B77**, 060506R(2008).
- [4] T. Shapoval, *et al.*, Phys. Rev. **B81**, 092505 (2010).
- [5] P.J. Cuadra-Solis, *et al.*, Physica **C468**, 777 (2008).

Spin waves in magnetic-semiconductor superlattices

J.P. Baltanás¹, D. Frustaglia¹

¹Dep. Física Aplicada II, Universidad de Sevilla, Spain.

Magnetic semiconductors are hybrid systems in which magnetic impurities couple indirectly via a bath of itinerant spin carriers [1,2]. The density of magnetic impurities can be modulated along the growth direction of the semiconductor to build periodic magnetic structures at the nanoscale, where quantum effects are relevant. Here [3], we present a theory of collective spin excitations in low-dimensional magnetic-semiconductor superlattices with a view to spin-wave band design for magnonics [4] (an emerging research field which explores spin waves, i.e. magnons, for information processing) and the possible development of interfaces with (spin)electronic systems.

[1] T. Jungwirth, J. Sinova, J. Mašek, J. Kučera, and A.H. MacDonald, *Rev. Mod. Phys.* **78**, 809 (2006).

[2] D. Frustaglia, J. König, and A.H. MacDonald, *Phys. Rev. B* **70**, 045205 (2004).

[3] J.P. Baltanás and D. Frustaglia, preprint (2011).

[4] V.V. Kruglyak, S.O. Demokritov, and D. Grundler, *J. Phys. D: Appl. Phys.* **43**, 264001 (2010); B. Lenk, H. Ulrichs, F. Garbs, and M. Münzenberg, *Phys. Rep.* **507**, 107 (2011).

Parimagnetism: Strongly Correlated Paramagnetism in RCo₂

M. Bonilla¹, J. Herrero-Albillos^{1,2}, I. Calvo¹, A. Figueroa¹, C. Castán¹,
J. A. Rodríguez- Velamazán^{1,3}, D. Schmitz⁴, E. Weschke⁴, D. Paudyal⁵, V. K. Pecharsky^{5,6},
K. A. Gschneidner Jr.^{5,6}, J. Bartolomé¹, L. M. García¹, and F. Bartolomé¹

¹Instituto de Ciencia de Materiales de Aragón y Departamento de Física de la Materia Condensada, CSIC - Universidad de Zaragoza, Pedro Cerbuna 12, 50009 Zaragoza, Spain.

²Centro Universitario de la Defensa de Zaragoza, Ctra. de Huesca s/n. 50.090 Zaragoza.

³Institute Laue Langevin, 38042 Grenoble, France

⁴Helmholtz-Zentrum Berlin, Albert Einstein strasse 15, 12489 Berlin (Adlershof), Germany

⁵Ames Laboratory, U.S. DOE, Iowa State University, Ames, Iowa 50011-3020, USA

⁶Department of Materials Science and Engineering, Iowa State University, Ames, Iowa 50011-2300, USA

A new magnetic configuration within the paramagnetic phase of ErCo₂ was proposed in 2007 as result of small angle neutron scattering (SANS), X-ray circular dichroism (XMCD) and ac susceptibility experiments. Within this magnetic configuration, coined as parimagnetism, the Co moments are disordered at the long-range but a net Co magnetic moment, antiparallel to the applied field (and to Er moment) is found, up to a certain temperature, T_f, well above T_c. The Co moment changes its orientation at T_f recovering the normal paramagnetic configuration. Short-range order between the Co atoms has been identified within this new magnetic configuration.[1]

Recently, transverse susceptibility (TS) and SANS measurements, performed above the ordering temperature of HoCo₂, allowed us to establish the existence of sizable magnetic short-range correlated regions. The correlation length obtained by SANS has an approximately constant value of $7.5 \pm 0.7 \text{ \AA}$ in the region of temperatures close to T_f and increases asymptotically to T_c. An XMCD study reveals the inversion of the Co net magnetization in HoCo₂, suggesting that parimagnetism is a more general phenomenon among the heavy lanthanide Co Laves phases. The temperature dependence of Co and Ho moments for different applied fields has been obtained from XMCD measurements, showing that rare earth moment also changes its orientation above T_f, giving rise to an entirely new magnetic configuration at high temperature. Indeed, based on TS measurements and our XMCD study we propose a new magnetic phase diagram for HoCo₂. First principles calculations based on LSDA+U approximation have also been performed in HoCo₂ to obtain insights on the origin of the Co-short-range correlated volume.

Work at Ames Laboratory is supported by US DOE under contract No.DE-AC02-07-CH11358. The authors acknowledge the support of IMANA and FEDER funds, neutron source ILL and photon source BESSY. C.M. Bonilla acknowledges Spanish MICINN.

[1] J. Herrero-Albillos, et al. Physical Review B 76, 094409, 2007.

"Dissipation in a coherently driven polariton fluid"

A. C. Berceanu, E. Cancellieri, F. Marchetti

Universidad Autonoma de Madrid

We study the superfluid properties of an intrinsically non-equilibrium system of coherently driven polaritons in the pump-only configuration. We analytically study the linear response of the system flowing against a point-like defect in the approximation of excitation close to the bottom of the lower polariton dispersion. Here, the spectral properties of the system collective excitations are uniquely determined by three parameters: the fluid velocity (normalised to the speed of sound), the interaction-renormalized pump detuning and the polariton lifetime [1]. We can distinguish two qualitatively different behaviours of the drag force exerted by the defect on the fluid as a function of the superfluid velocity: For positive or zero detuning, similarly to what happens in equilibrium systems, the crossover from supersonic to subsonic behaviour is determined by a critical velocity which equals the speed of sound, while the critical velocity determining the crossover for negative detuning is always bigger than the speed of sound. In both cases, we find the drag in the subsonic regime to be solely a consequence of the non-equilibrium nature of the system and not due to non-linear effects induced by the defect size. We show the drag to have a linear behaviour as a function of polariton lifetime, in agreement with previous numerical studies of the fully non-linear problem [2].

[1] C. Ciuti and I. Carusotto, *Physica Status Solidi B* 242, 2224 (2005).

[2] E. Cancellieri et al., *Phys. Rev. B* 82, 224512 (2010).

Magnetic inhomogeneities and spin torque studies by low and high frequency noise in sub-100nm magnetic tunnel junctions

J.P. Cascales^{1,*}, D. Herranz¹, F.G. Aliev¹, U.Ebels², J. Katine³

¹Departamento Física de la Materia Condensada, C03, Universidad Autónoma de Madrid, 28049 Madrid, Spain

²2SPINTEC, UMR 8191, CEA/CNRS/UJF, INAC, 38054 Grenoble Cedex, France

³. Hitachi Global Storage Technologies, San Jose, CA 95135 USA

Magnetic tunnel junctions consist of two ferromagnetic electrodes separated by an insulating barrier, through which electrons tunnel or not depending on their spin. These structures exhibit tunnel magnetoresistance and are used as magnetic sensors. Improving MTJs and characterizing the physical phenomena that take place in the devices is essential for a better technological application, as well as interesting from a fundamental point of view. One way of doing this is by measuring the electronic and magnetic fluctuations (or noise) that occur in MTJs [1].

We present an experimental setup where electronic noise in nanoscale (diameter of 100nm or less) elliptical magnetic tunnel junctions is measured at room temperature. The setup allows measurements to be made in two different ranges of frequency: from a few Hz to 100kHz and between 10MHz and 20 GHz. This work constitutes the first detailed comparative study of TMR, low frequency (1/f and random telegraph noise) and high frequency noise on the same MTJ samples.

A transition from thermal ferromagnetic resonance to spin-transfer torque phenomena is measured at high frequencies. Even clearer signs of the transition are detected in low frequency noise measurements for the same values of external magnetic field and applied current densities (around 10^7 A/cm²). A qualitative model is described in order to explain the results.

Also, random telegraph noise (RTN) due to magnetic inhomogeneities has been detected and investigated in these small junctions through low frequency measurements by analyzing both noise power spectra and resistance time series. For certain external magnetic field values, close to a transition in the magnetic configuration, the spectra show a Lorentzian-like type dependence and the time series of the noise undoubtedly exhibit random voltage jumps between two states (which is the definition of RTN). This way, the presence of RTN is clearly identified. One can also estimate the fluctuating magnetic moment responsible for the noise and its dependence with the applied current, in the region where spin torque effects become important.

[1] D. Herranz, A.Gomez-Ibarlucea, M. Schäfers, A.Lara, G.Reiss, F.G. Aliev, Applied. Physics Letters, **99**, 062511 (2011).

Disorder and Magnetism in Bilayer Graphene

E. V. Castro, M. P. López-Sancho, and M. A. H. Vozmediano

Instituto de Ciencia de Materiales de Madrid-CSIC, C/ Sor Juana Inés de la Cruz 3, 28049-Madrid, Spain.

One of the most interesting aspects of graphene for the applications concerns the magnetic properties which, by now, are not well understood. Room-temperature ferromagnetic features have been experimentally observed in defective graphite, related to defect structures¹ and in graphene samples². There are as well experimental results claiming that no room-temperature magnetic interactions are detected at graphite surface steps³ or the absence of ferromagnetism down to a temperature of 2K in graphene samples⁴. It seems clear by now that disorder, such as defects, edges, vacancies or voids, induce zero-energy states⁵, and that the underlying mechanism leading to magnetism in these carbon structures is related to the existence of unpaired spins at defects induced by a change in the coordination of the carbon atoms³.

In this work the magnetic properties of vacancy-induced localized states are investigated in bilayer graphene. There are two different zero energy states associated to the two inequivalent vacancies that can appear in the Bernal stacking of graphene layers⁶. These two zero energy states give rise to two different spin polarized local states. The possibility offered by the bilayer graphene of opening an energy gap in the spectrum by applying an electric field, introduces the capability of tuning polarization of the system for experimentally accessible gate voltages⁷. The most interesting case arises in the presence of a gate opening a gap when considering two vacancies of the same sublattice located at different layers. We have shown that with realistic values of the parameters and for experimentally accessible gate voltages we can have a magnetic switching between an unpolarized and a fully polarized system⁸. Further control over the magnetic properties of bilayer graphene is achieved by applying pressure in the perpendicular direction⁹.

[1] J. Cervenka, M. I. Katsnelson, and C. F. J. Flipse, *Nature Physics* **5**, (2011) 840.

[2] Y. Wang *et al*, *Nano Letters*, **9**, (2009) 220.

[3] D. Martínez-Martín, M. Jaafar, R. Pérez, J. Gómez-Herrero and A. Asenjo, *Phys. Rev. Lett.* **105**, (2010) 257203

[4] M. Sepioni, *et al*, *Phys. Rev. Lett.* **105**, (2010) 207205.

[5] N. M. Ugeda, I. Brihuega, F. Guinea, and J. M. Gómez-Rodríguez, *Phys. Rev. Lett.* **104**, (2010) 096804.

[6] E. V. Castro, M. P. López-Sancho, M. A. H. Vozmediano, *Phys. Rev. Lett.* **104**, (2010) 036802.

[7] E. V. Castro, N. M. R. Peres, T. Stauber, N. A. P. Silva, *Phys. Rev. Lett.* **100**, (2008) 186803.

[8] E. V. Castro, M. P. López-Sancho, M. A. H. Vozmediano, *New J. of Physics* **11**, (2009) 095017.

[9] E. V. Castro, M. P. López-Sancho, M. A. H. Vozmediano, *Phys. Rev. B* **84**, (2011) 075432.

Doping level of GAN: si nanowires studied by C-AFM and photoluminescenceR. Mata¹, J. Martínez-Pastor¹, B. Daudin², and A. Cros^{1*}

¹Materials Science Institute, University of Valencia, Po. Box 22085, E46071 Valencia, SPAIN

²CEA-CNRS group « Nanophysique et Semiconducteurs », Institut Néel/CNRS-Univ. J. Fourier and CEA Grenoble, INAC, SP2M, 17 rue des Martyrs, 38 054 Grenoble, FRANCE

Due to their direct band-gap and high thermal stability, nitride semiconductors (InN, GaN, AlN and their alloys) are well suited for the development of optoelectronic devices covering a large spectral range, from the infrared to the ultraviolet. In the form of nanowires, these materials can be grown strain and dislocation free on Si wafers, allowing their integration with the silicon based electronics.

In this work we have investigated the optical and electronic properties of GaN nanowires grown by Molecular Beam Epitaxy and doped with different concentrations of Si. The nanowires are grown directly on highly *n*-doped Si wafers [1]. Due to the short size of the nanowires (~ 250-300 nm length, 10-25 nm diameter), the determination of the mobility and electron concentration through Hall measurements is not possible. Instead, we have used Conductive Atomic Force Microscopy at room temperature in order to study the electrical characteristics of single nanowires [2]. As the Si content increases, the characteristic I-V curves display a transition from Schottky to Ohmic behaviour. After a statistical study of the results within each sample, the analysis of the I-V curves allows estimating the density of *n*-type carriers in the different samples. The results obtained are consistent with an increase of Si content as the Si cell temperature increases. Additionally, photoluminescence measurements have been carried out. The samples with the lowest Si content present a peak characteristic of the donor-acceptor pair emission. Other peaks are attributed to electronic transitions induced by the increase of free carrier concentration in the nanowires [3,4]. The PL emission of the nanowire sample with highest doping level shows a blue shift and a broadening of the main emission peak which is related to band-filling effects. Band shifts related to structural changes induced by doping can be ruled out by Raman scattering except for the sample with the highest Si content, where a blue shift of the phonon modes is observed [4,5].

[1] R. Mata, K. Hestroffer, J. Budagosky, A. Cros, C. Bougerol, H. Renevier, B. Daudin **334**, (2011) 177.

[2] B. Pérez-García, J. Zúñiga-Pérez, V. Muñoz-Sanjosé, J. Colchero, and E. Palacios-Lidón, *Nano Letters* **7**, (2007) 1505.

[3] E. F. Schubert, I. D. Goepfert, W. Grieshaber, and J. M. Redwing, *Applied Physics Letters* **71**, (1997) 921.

[4] F. Furtmayr, M. Vielemeyer, M. Stutzmann, A. Laufer, B. K. Meyer, and M. Eickhoff, *Journal of Applied Physics* **104**, (2008) 074309.

[5] J. Sánchez-Páramo, J. M. Calleja, M. A. Sánchez-García, and E. Calleja, *Applied Physics Letters* **78**, (2001) 4124.

Efecto magnetocalórico en multicapas Gd/Ti

D. Doblas^{1,*}, V. Franco¹, A. Conde¹, A.V. Svalov^{2,3}, G.V. Kurlyandskaya^{2,3}

¹Dpto. Física de la Materia Condensada, ICMSE-CSIC, Universidad de Sevilla. Apdo. 1065. 41080-Sevilla, España

²Dpto. Electricidad y electrónica, Universidad del País Vasco. 48080-Bilbao, España

³Ural Federal University, 620083, Ekaterinburg, Russia.

El efecto magnetocalórico consiste en la variación reversible de la temperatura de un material magnético al ser imanado/desimanado adiabáticamente. Este efecto ha atraído un notable interés de la comunidad científica en los últimos años por su posible aplicación en la refrigeración magnética a temperatura ambiente, ya que ésta es energéticamente más eficiente que los refrigeradores basados en la compresión/expansión de gases, y es más respetuosa con el medio ambiente al no emplear gases que alteren la capa de ozono o provoquen efecto invernadero.

Para que un refrigerador magnético sea viable para aplicaciones domésticas, el campo magnético aplicado en el mismo debe encontrarse en el rango $H=1,5 - 2$ T. Por lo tanto, es de gran importancia optimizar la respuesta de los materiales magnetocalóricos al campo magnético aplicado, especialmente en el rango de H moderados. Además, los dispositivos electrónicos requieren un material refrigerante en forma de película delgada debido a su mayor compatibilidad con los circuitos electrónicos y mínimo peso de dispositivo [1].

En la mayoría de prototipos de refrigerador actuales, el material magnetocalórico empleado es el Gd, debido a la ausencia de histéresis térmica y magnética. Recientemente se ha puesto de manifiesto que el diseño de multicapas de NiCu con diferentes composiciones de las capas (y, por tanto, con diferentes temperaturas de Curie) permite controlar la dependencia con H del efecto magnetocalórico, optimizando la respuesta del material para campos moderados [2]. Sin embargo la composición de dichas fases impide obtener valores de la respuesta magnetocalórica aplicables en la práctica. En este trabajo se demuestra que la fabricación de multicapas Gd/Ti es un método adecuado para mantener la respuesta magnetocalórica del material dentro de valores utilizables en la práctica, a la vez que permite incrementar la dependencia con el campo H cuando se compara con la respuesta del Gd masivo.

Este trabajo ha sido financiado por el Ministerio de Ciencia e Innovación y EU FEDER (Proyectos MAT 2010-20537 y MAT2008-06542-C04_02), el PAI de la Junta de Andalucía (Proyecto FQM-6462), la United States Office of Naval Research (Proyecto N00014-11-1-0311).

[1] A. V. Svalov, V. O. Vas'kovskiy, J. M. Barandiarán, K. G. Balymov, I. Orue, G. V. Kurlyandskaya, *Physica Status Solidi A*, 208 (2011) 2273.

[2] R. Caballero-Flores, V. Franco, A. Conde, L.F. Kiss, L. Péter, I. Bakonyi. *J. Nanosci. Nanotech.* (aceptado para publicación).

Photoluminescence of Single ZnOTetrapods

L. C. Fernandes-Silva^{1,*}, M. D. Martín¹, H. P. Van der Meulen¹, L. Kłopotowski², J. M. Calleja¹ and L. Viña¹

¹ Departamento de Física de Materiales, Universidad Autónoma de Madrid, E-28049 Madrid, Spain

² Polish Academy of Sciences, Institute of Physics, Warsaw, Poland

ZnO is one of the most attractive wide band-gap phosphor materials with a direct band gap of 3.37 eV and a large exciton binding energy (60 meV), which allows UV lasing action to occur at room temperature [1]. Among various ZnO structures, tetrapods are of particular interest [2] because they possess remarkable optical, electronic and mechanical properties.

In this work we present the emission spectra of individual crystalline pure ZnO tetrapods (inset of figure 1), measured both by time-resolved and time-integrated photoluminescence (PL) spectroscopy as a function of temperature, from 13K to room temperature and pump power, from 280-1000 μ W, paying special attention to the dynamics.

We observe that at room temperature the photoluminescence spectra are dominated by the free exciton recombination. The power-dependence results show that the luminescence intensity increases with power and a red-shift occurs at high powers due to carrier heating. In the temperature dependence for a constant power, we observe a blue-shift of the free exciton emission at decreasing the temperature (figure 1). At low temperatures the PL spectra show both surface and bulk bound excitons. Concerning the dynamics study we observe that the emission energy of the bound excitons transitions does not change with time, for all temperatures. We have tentatively fitted the decaying part of the bound excitons PL intensity with a single exponential function, extracting a decay time. We find that this decay time increases with increasing temperature, evidencing an enhancement of the non-radiative recombination mechanisms.

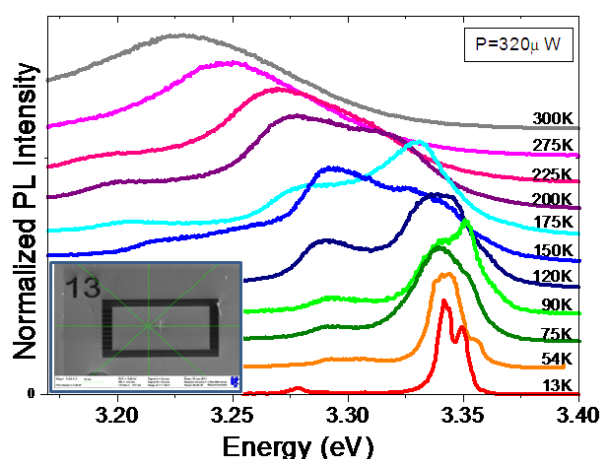


Figure 1. Temperature dependence of the normalized PL intensity versus the energy. The inset shows a SEM image of the studied tetrapod.

[1] Nguyen ThiThucHien, DoanManh Ha, Ngo Xuan Dai, Nguyen Thi Thu Huong, VNU Journal of Science, Mathematics - Physics 24 (2008) 24-29; Zhong Lin Wang, Materials Today, June (2004).

[2] V.V. Zanamai, et al., Appl. Phys. B 99 (2010) 215-222.

Amorphous SiO_xN_y thin films with controlled closed porosity and its effects on refractive index and mechanical properties.

V. Godinho, T.C. Rojas, A. Fernández*.

Instituto de Ciencia de Materiales de Sevilla (CSIC-Univ. Sevilla), Avda. Américo Vespucio nº 49, 41092. Sevilla

Amorphous silicon oxynitride coatings with similar composition and different closed porosity were prepared by magnetron sputtering. Pores shape and distribution were evaluated by scanning electron microscopy and transmission electron microscopy.

Different target to substrate distances can be used to control not only pore size, as can be seen in fig 1, but also the volume fraction of pores introduced in the coatings.

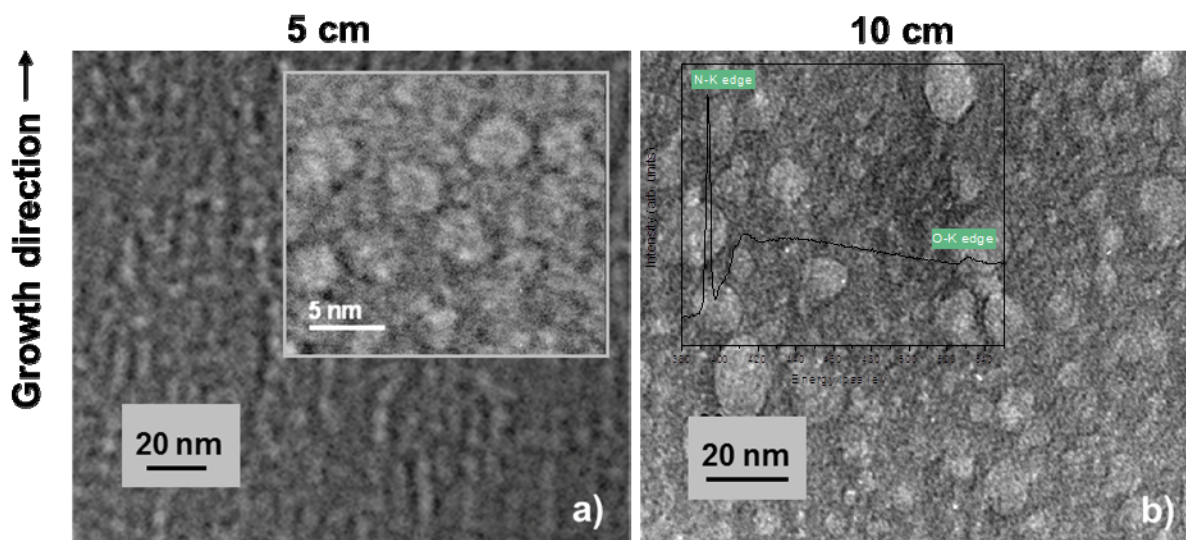
A substantial decrease in the refractive index of these coatings is achieved by controlled introduction of closed porosity.

Raman and Electron Energy Loss Spectroscopy (EELS) analysis proved that the pores are filled with molecular nitrogen trapped during deposition.

The mechanical properties evaluated by nanoindentation show that the presence of closed porosity does not compromise the mechanical integrity of these coatings.

As a conclusion, the introduction of closed porosity with molecular N_2 trapped inside allows not only have thin films with different dielectric constant but also to keep the good mechanical properties typical of silicon oxynitride coatings [1]. The easiness of the deposition method allows scaling up to industrial processes, making these coating very interesting for different applications.

Fig.1 TEM images of the sample prepared at different substrate-target distances. EELS spectra (N and O K-edges) measured inside a pore (left inset).



[1] V. Godinho, T. C. Rojas and A. Fernández
Microporous & Mesoporous Materials 149 (2012) 142-146

Time Dependent Density Functional Theory total energy calculations using numerical atomic orbitals.J.J. Fernández^{1,*}, P. García-González², J.E. Alvarelos¹

¹Universidad Nacional de Educación a Distancia, Departamento de Física Fundamental, 28040 Madrid, Spain.

²Universidad Autónoma de Madrid, Departamento de Física Teórica de la Materia Condensada, 28049 Madrid, Spain.

Although time-dependent density functional (TD-DFT) theory is mainly used to calculate the excitation properties of electronic systems, it is also a powerful methodology to obtain their ground state properties of these systems. In this work we present some preliminary results of a project focused on the study of the ground state properties by means of an implementation of the TD-DFT in terms of a representation of the wave function in terms of a basis set of numerical atomic functions.

We are going to present some detailed calculations of the ground state exchange and correlation energies of a set of atoms, ions and molecules. The exchange energy will be calculated by means of the Fock double integral over occupied orbitals. For the correlation energy we will focus our work in the use of the Adiabatic-Connection Density-Fluctuation Theorem and we will obtain the correlation energy using different approximations to the exchange-correlation TD-DFT kernel (RPA, PGG, DW, ...) and some corrections based on the density (RPA+). In order to assess the results we have also calculated the correlation energy using perturbation theory at the MP2 level.

Interferences and modulation of Surface plasmons in thin metallic films

F. Galvez^{1,*} and M. A Garcia²

¹Dpt. Material Physics, University Complutense at Madrid, Spain

²Institute for Ceramic and Glass, CSIC & IMDEA Nanociencia, Madrid, Spain

Surface plasmons resonance (SPR) is the most remarkable property of metallic surfaces. It consists on a collective oscillation of the conduction electrons at the metal-dielectric interface that can be excited upon illumination with coherent light. The excitation of (SPR) requires the incident light matching the dispersion relation of SPR, that can be achieved upon particular geometric conditions. SPR increases locally the electric fields up to 2 orders of magnitude and is strongly sensitive to any modification in the metallic film or the surrounding media

In this work, we present a set of experiments where two lasers are focused on the surface of a metallic film, one of them in the resonant conditions. We show how the excitation of SPR by one of the lasers can be modified by the illumination with the second one providing a method to modulate the SP with the light in non-resonant conditions. The effects of lasers intensity, wavelength and incidence angle (that is, effective wavevector) are studied.

Epitaxial magnetoplasmonic structures exhibiting enhanced surface-plasmon-polariton wave vector magnetic modulation

M. Iglesias¹, E. Ferreiro-Vila², E. Paz¹, F. J. Palomares¹, F. Cebollada³, J. M. González⁴, G. Armelles², J. M. García-Martín², and A. Cebollada²

¹Instituto de Ciencia de Materiales de Madrid (CSIC), Sor Juana Inés de la Cruz 3, E-28049 Madrid, Spain

²IMM-Instituto de Microelectrónica de Madrid (CNM-CSIC), Isaac Newton 8, PTM, E-28760 Tres Cantos, Madrid, Spain

³POEMMA, Departamento de Física Aplicada a las T.I., Universidad Politécnica de Madrid, E-28031 Madrid, Spain

⁴Unidad Asociada ICMM-CSIC/IMA-UCM, Sor Juana Inés de la Cruz 3, E-28049 Madrid, Spain

We report on the magnetoplasmonic properties of Au/Fe/Au trilayers deposited on top of single crystalline MgO substrates by using a pulsed laser ablation deposition [1]. A series of samples having constant Au layers thicknesses (9 nm) and different Fe layer thicknesses in the range from 1 up to 6 nm, were structurally and morphologically characterized by means of X-ray diffraction/reflectivity and atomic force microscopy. The so-obtained data evidenced both the occurrence of epitaxial growth and that of ultraflat surfaces having average (rms) roughnesses of the order of 0.1 nm. The measurement of the surface plasmonic resonance effects on the magneto-optical activity of the samples allowed us to quantify the applied magnetic field induced surface-plasmon-polariton wave vector modulation which reached values of the order of $4 \times 10^6 \Delta k/k$ for Fe thicknesses maximizing the magneto-optical activity (i.e.: ca. 5 nm). This result supports the feasibility of implementing optimized active plasmonic devices using these structures [2].

[1] E.Ferreiro-Vila et al., Phys. Rev. B 83, 205120 (2011)

[2] V. Temnov et al., Nature Photonics 4, 107 (2010)

Study of the transport properties in two dimensional topological insulators in presence of disorder

D. Gosálbez-Martínez^{1,*}, J. Fernández-Rossier^{1,2}, J.J. Palacios³

¹Universidad de Alicante, Departamento de Física Aplicada, Ctra. San Vicente del Raspeig, s/n. 03690 - San Vicente del Raspeig. Alicant, Spain.

²International Iberian Nanotechnology Laboratory, Av. Mestre José Veiga 4715-310 Braga, Portugal.

³Universidad Autónoma de Madrid, Departamento de Física de la Materia Condensada, Facultad de Ciencias, C03 Campus de Cantoblanco Madrid 28049, Spain.

Two dimensional topological insulators present gapless spin filtered edge states which are topologically protected against backscattering. As long as disorder does not mix the states of opposite edges or with bulk ones, these states contribute to the two terminal conductance as a single quantum channel regardless of the amount of non-magnetic disorder present in the sample. We address this problem for two different materials that have been predicted to present the quantum spin Hall insulator phase, graphene^[1] and a bilayer of Bi(111)^[2]. We describe their electronic structure using an orthogonal tight-binding model in the Slater-Koster approximation including the intra-atomic spin-orbit interaction. The conductance is computed using the Landauer formula making use of the ALACANT transport package^[3]. We study the effect of different types of disorder as Anderson disorder, edge vacancies and edge reconstruction in both systems.

References

- [1] C.L. Kane and E. J. Mele, Phys. Rev. Lett. **95**, 226801 (2005), C.L. Kane and E. J. Mele, Phys. Rev. Lett. **95**, 146802 (2005).
- [2] Shuichi Murakami, Phys. Rev. Lett. **97**, 236805 (2006).
- [3] Alicante Atomistic Transport Computation Applied to NanoTransport (ALACANT) software package. (<http://alacant.dfa.ua.es/index.html>).

Low frequency noise due to magnetic inhomogeneities in submicron FeCoB/MgO/FeCoB magnetic tunnel junctions

D.Herranz¹, A. Gomez-Ibarlucea¹, A. Lara¹, M. Schäfers², G. Reiss², and F.G. Aliev¹

(1) Dpto. Física Materia Condensada, CIII, Universidad Autónoma de Madrid, 28049, Cantoblanco, Madrid Spain

(2) Dept. of Physics, University of Bielefeld, Bielefeld 33615, Germany

The discovery of tunneling magnetoresistance (TMR) exceeding 100% at room temperature has boosted scientific and technological interest in MgO based magnetic tunnel junctions (MTJs). Submicron-sized, exchange-biased MTJs with FeCoB electrodes have recently become basic elements in spin torque devices. We investigate TMR and low frequency noise (from few Hz to few kHz) as a function of external magnetic field and bias voltage at room temperature, in elliptic submicron FeCoB/MgO/FeCoB [1] with areas between 0.0245 and $0.117\mu\text{m}^2$ [2]. We have observed that the TMR and low frequency noise in submicron MTJs as a function of the area of the samples, are strongly affected by magnetic inhomogeneities/domain walls (MI/DWs).

In the smallest junctions ($A=0.0245\text{-}0.0503\mu\text{m}^2$), we have found an unexpected random telegraph noise (RTN1), deeply in the parallel state, accompanied by an extremely small change in resistance of about 0.1%. This noise is weakly influenced by the external bias and is probably due to stray field induced MI/DWs in the hard layer (Fig.1).

The second noise source (RTN2) is observed in the antiparallel state for larger junctions ($A=0.0565\text{-}0.0675\mu\text{m}^2$), shown in Fig. 2. The strong asymmetry of RTN2 with current and the insignificance of the self-field indicate spin torque acting on the MI/DWs in the soft layer at current densities below $5\times 10^5\text{ A/cm}^2$.

These results could allow the development of new devices based on magnetic tunnel junctions with control over domain wall motion using low current densities.

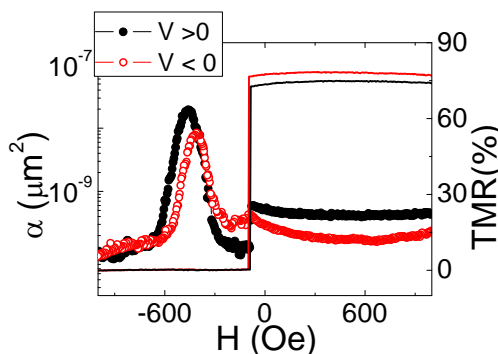


Fig. 1 Hooge and TMR vs H at $J=1.9\times 10^6\text{ A/cm}^2$ for MTJs with $A=0.0245\mu\text{m}^2$.

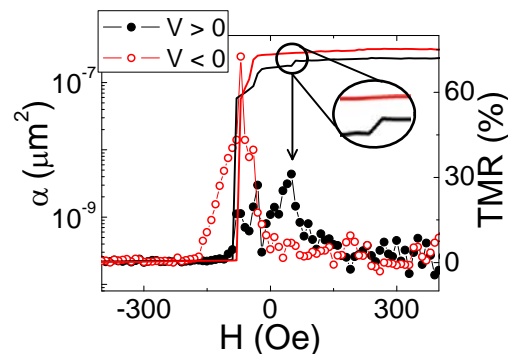


Fig. 2 Hooge and TMR vs H at $J=5.2\times 10^5\text{ A/cm}^2$ for MTJs with $A=0.0675\mu\text{m}^2$. The resistance step (remarked by black circle) influences the low frequency noise at $V > 0$ and not present at $V < 0$.

[1] W. Skowroński, et al., JAP, **107**, 093917 (2010)

[2] D. Herranz, et al., Appl. Phys. Lett., **99**, 062511 (2011).

MFM characterization of double-vortex metastable state in circular Permalloy dots

O. Iglesias-Freire^{1,*}, A. Lara², A. Awad², M. Jaafar^{1,2}, V. Metlushko³, A. Asenjo¹ and F.G. Aliev²

¹Instituto de Ciencia de Materiales de Madrid (ICMM-CSIC), 28049 Madrid (Spain)

²Dpto. Física de la Materia Condensada, C03, Universidad Autónoma de Madrid, 28049 Madrid (Spain)

³Department of Electrical & Computer Engineering, University of Illinois at Chicago, Chicago, IL, 60607 (USA)

In the last decade the magnetic vortex state in circular magnetic dots has attracted increasing interest due to the possibility of its implementation in new types of high density storage media, logic operation devices or spin-polarized current driven spintronic devices. The existence of a long-living intermediate metastable double-vortex state [1,2] below some critical thickness, around 25 nm for Permalloy dots with diameters of 1000 nm, was suggested. In this work, the magnetization reversal processes involving the nucleation of magnetic vortices in Py dots is characterized by using a MFM-based technique [3] under variable magnetic fields [4]. Two Py dots samples with the same diameter (1000 nm) and different thickness 50, 20 nm have been studied.

In this communication we present results which confirm the existence of a long-living double-vortex metastable state in 20 nm thick dots. Using a MFM-based method, we have been able to unravel the position of the two vortices for a wide range of applied fields and their transition into a single vortex configuration. Furthermore, we have obtained quantitative information about the vortex nucleation and annihilation fields measured in a single dot. Different behavior, however, was obtained in 50 nm thick dots where direct nucleation of a single vortex is observed. In addition, micromagnetic calculations using OOMMF [5] show good agreement with the MFM images and comparing the MFM contrast and the simulation permits to correlate the magnetization configuration and to understand the evolution of the double vortex configuration in field.

In summary, the metastable double-vortex state in Py dots, as well as the critical fields are characterized experimentally using MFM. Numerical simulations support main observations.

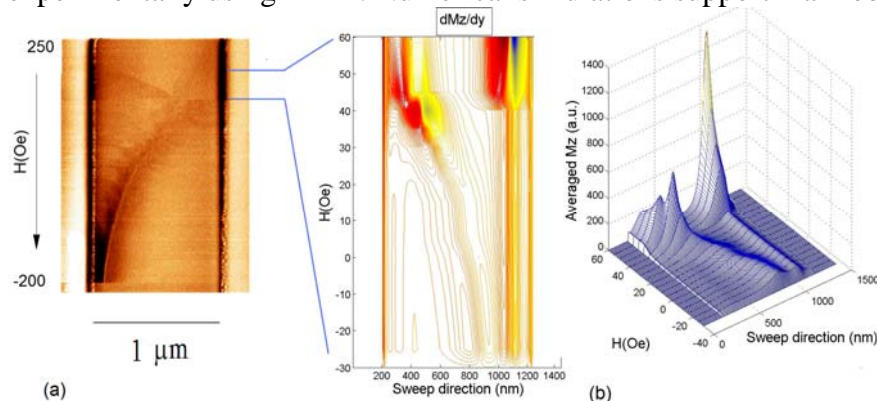


Figure. (a) MFM-based image (MFM signal along the x axis versus the externally applied magnetic field) of a Py dot showing the transition from a double-vortex into a single vortex state. (b) & (c) OOMMF simulation of these processes.

[1] F.G. Aliev, et al., Proceedings of International Conference on Electromagnetics in Advanced Applications (ICEAA2010), IEEE-Explore, 160 (2010).

[2] F.G. Aliev, et al., Phys. Rev. B84, 144406 (2011).

[3] M. Jaafar, et al., Nanoscale Research Letters 6, 407 (2011).

[4] M. Jaafar, et al., Ultramicroscopy 109, 693 (2009).

[5] <http://math.nist.gov/oommf/>

Magnetocaloric effect in $\text{Fe}_{77}\text{Co}_{5.5}\text{Ni}_{5.5}\text{Zr}_{7-z}\text{X}_z\text{B}_4\text{Cu}_1$ ($\text{X} = \text{Nb}, \text{Hf}$) soft magnetic amorphous alloys

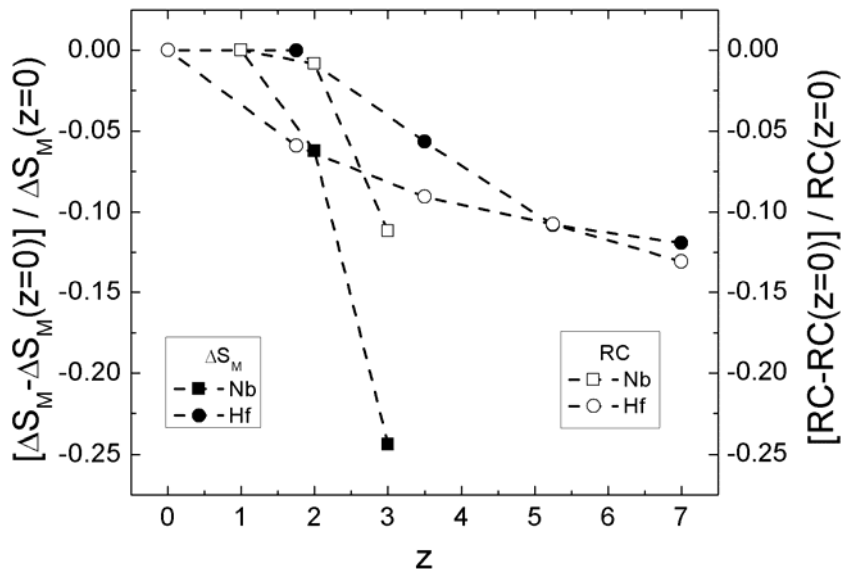
B. Ingale^{1,*}, V. Franco¹, A. Conde¹, K. E. Knipling², M. A. Willard²

¹Dpto. Física de la Materia Condensada, ICMSE-CSIC, Universidad de Sevilla. Apdo. 1065. 41080-Sevilla, España

²Multifunctional Materials Branch. U.S. Naval Research Laboratory. 4555 Overlook Ave. SW, Washington, District of Columbia 20375, U.S.A.

There is a growing interest in studying the applicability of soft magnetic amorphous alloys for magnetic refrigeration due to their tunable magnetic transition temperatures by alloying and significantly reduced magnetic as well as thermal hysteresis, in contrast to the materials that undergo first order magneto-structural transitions. Moreover, refrigerant capacities of this kind of materials can be comparable, or even larger, than those of well-known giant magnetocaloric materials [1].

In this work, we have studied the magnetocaloric effect in the series of $\text{Fe}_{77}\text{Co}_{5.5}\text{Ni}_{5.5}\text{Zr}_{7-z}\text{X}_z\text{B}_4\text{Cu}_1$ ($\text{X} = \text{Nb}$ and Hf) melt-spun alloys (~ 3 mm wide and $\sim 20\mu\text{m}$ thick) with compositions $z = 0, 1.75$ and 3.5 for Nb while $z = 0, 1.75, 3.5, 5.25$ and 7.0 for Hf. The magnetic entropy change, ΔS_M , decreases with the substitution of Zr by Nb or Hf, causing Nb a larger decrease. The refrigerant capacity, RC, is also negatively affected by these substitutions, being the decrease in RC comparable for both elements. The figure shows the relative variation of these two magnitudes with the compositional changes.



This work was supported by the Spanish Ministry of Science and Innovation and EU FEDER (Project MAT 2010-20537), the PAI of the Regional Government of Andalucía (Project FQM-6462), and the United States Office of Naval Research (Projects N00014-11-1-0311 and N0001410WX30490).

[1] R. Caballero-Flores, V. Franco, A. Conde, K. E. Knipling, and M. A. Willard, Applied Physics Letter **96**, (2010) 182506.

Tailored luminescent emission of dyes embedded in porous resonators

Alberto Jiménez-Solano^{1*}, José Miguel Luque¹, Mauricio E. Calvo¹, Fernando Fernández-Lázaro², Hernán Míguez¹

¹ Instituto de Ciencia de Materiales de Sevilla (CSIC), Américo Vespucio, 49 41092 Sevilla, Spain.

² Universidad Miguel Hernández de Elche, Av. de la Universidad s/n, 03202 Elche, Spain.

Here we study the light emitted from different hybrid organic dye doped inorganic nanoparticle-based one dimensional (1D) photonic crystal (PC) architectures. The increase in the photon density of states caused by confinement in very specific slabs of the multilayer implies a lower photon group velocity,[1] which in turn yields longer light-matter interactions. We investigate both experimentally and theoretically[2] how the angular distribution of light emitted from these 1DPC structures is modified depending on the spectral matching of either resonant or stop band modes of the PC. Our measurements are explained in terms of the electromagnetic field distribution in the photonic structure. These results prove that by changing the photonic environment of a dye, it is possible to finely tune its optical response throughout the visible.

References

[1] Bendickson, J. M.; Dowling, J. P.; Scalora, M. *Phys. Rev. E*, **1996**, 53, 4107.

[2] Lozano, G.; Colodrero, S.; Caulier, O.; Calvo, M.E.; Míguez, H. *J. Phys. Chem. C*. **2010**, 114, 3681.

Spin waves along domain walls in triangular and circular Py dots with vortices

A. Lara^{1,*}, A. Awad¹, F.G. Aliev¹, V. Metlushko²

¹ Dpto. Física Materia Condensada, C03, Universidad Autónoma de Madrid, Cantoblanco, 28949, Madrid, Spain

² University of Illinois at Chicago, Department of Electrical & Computer Engineering, Chicago, IL, USA

Recently there has been increasing interest in magnetic dots in the vortex state. They have been suggested as a potential new way to the creation of nanoscale memory and spin torque vortex oscillators. Although excitations of the confined domain walls (DW) or single vortex (SV) states are understood, the nature of the spin waves involving both vortices and DWs remains unclear.

We have investigated the magnetization dynamics of Permalloy samples, by means of broadband ferromagnetic resonance technique and micromagnetic simulations, observing a good agreement between them for modes shifting and splitting. We have observed recently a new type of quasi one dimensional spin wave modes along the DWs connecting the vortices and edge half-antivortices present in the double magnetic vortex state (DMV), a metastable state that can be found in circular dots [1]. A new study has been carried out in 25 nm thick Py triangles (see Fig. 1), and we have detected several modes of the same kind up to 14 GHz. In this case the domain walls naturally appear in the SV state (ground state), connecting the vortex core and the vertices of the triangle. We can simulate the spin waves profile as a function of time for each mode. These spin waves are analogous to the displacement waves of strings and could be excited in a wide class of nanostructures possessing domain walls, which could be interesting for studying the dependence of the modes on the symmetry and geometry of the dots.

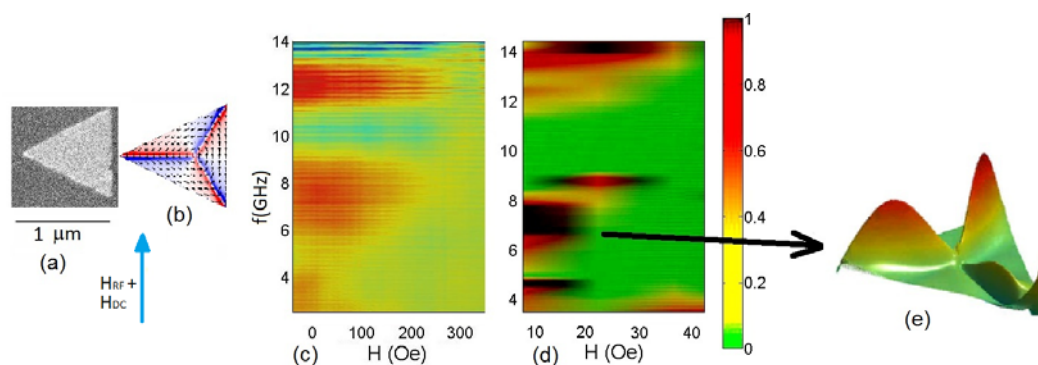


Fig. 1: (a) SEM image of triangular magnet. (b) Simulated magnetization and domain walls in ground state. Direction of applied fields given by blue arrow (c) Measured dynamic response at different static fields. (d) Simulated response (static fields don't necessarily match since we don't know parameters like the damping). (e) M_x amplitude profile at 6.6 GHz. Highest amplitude at the domain walls.

[1] F. G. Aliev, A. A. Awad, D. Dieleman, A. Lara, V. Metlushko, and K. Y. Guslienko, *Physical Review* **B84**, 144406 (2011).

Supported AgNPs@ZnO Nanorods by low temperature PECVDM. Macias-Montero^{1,*}, Z. Sagui², A. R. Gonzalez-Elipe¹, A. Borrás¹

¹ Instituto de Ciencia de Materiales de Sevilla (ICMS, CSIC-US), Nanotechnology on Surfaces Lab., address, country

² Department of Materials Science and Metallurgy University of Cambridge, Pembroke Street, CB2 3QZ, Cambridge (United Kingdom)

³ BIONAND (Andalusian Centre for Nanomedicine and Biotechnology), Parque Tecnológico de Andalucía, c/ Severo Ochoa, 35, 29590 Campanillas, Málaga, Spain

Abstract.-

In this communication we report on a new type of 1D nanostructures consisting of supported hollow ZnO nanorods (NRs) decorated with Ag nanoparticles (NPs) fabricated by low temperature plasma enhanced chemical vapor deposition (PECVD). The 3D reconstruction by high-angle annular dark field scanning transmission electron microscopy (HAADF-STEM) electron tomography reveals that the Ag NPs are distributed along the hollow interior of highly porous ZnO NRs. Supported and vertically or tilted aligned Ag-NPs@ZnO-NRs grow at 135 °C by PECVD of the Zn precursor on heterostructured substrates fabricated by sputtered deposition of silver on flat surfaces of Si wafers, quartz slides or ITO. Tuning the deposition angle Ag@ZnO NRs depicting tilting angles from 50° to 90° can be homogeneously growth. Following this idea zig-zag nanostructures are also fabricated by modification of the growth angle during the deposition. The growth mechanisms of these structures and their wetting behavior prior and after visible light irradiation are as well critically discussed. Thus, the as prepared surfaces are superhydrophobic with water contact angles higher than 150°. These surfaces turn into superhydrophilic with water contact angles lower than 10° after prolonged irradiation under both visible and UV light. The evolution rate of the wetting angle and its dependence on the light characteristics are related with the nanostructure and the presence of silver embedded within the ZnO NRs.

*** Corresponding author:**

D. Manuel Macías Montero

Email: manuel.macias@icmse.csic.es

Growth of SiO₂ Thin Films by Plasma-Assisted Reactive Magnetron Sputtering Under the Impingement of Positive and Negative Ions

M. Macias-Montero^{1*}, F.J. Garcia-Garcia¹, R. Álvarez¹, J. Gil-Rostra¹, F. Yubero¹, A. R. Gonzalez-Elipe¹, A. Palmero¹, J. Cotrino^{1,2}

¹Instituto de Ciencia de Materiales de Sevilla, c/ Américo Vespucio 49, 41092 Seville, Spain

² Universidad de Sevilla, Departamento de Física Atómica, Molecular y Nuclear, Av. Reina Mercedes s/n, 41012 Seville, Spain

Preference: Poster presentation.

Abstract.-

Growth of amorphous SiO₂ thin films deposited by reactive magnetron sputtering has been studied under different oxygen partial pressures at low temperatures. Film microstructures varied from coalescent vertical column-like to compact microstructures, possessing all of them similar refractive indexes. A discussion on the process responsible for the different microstructures is carried out, focusing on the influence of i) surface shadowing mechanism, ii) positive ion impingement on the film, and iii) negative ion impingement. We conclude that only the latter can be responsible for the obtained microstructural changes, and, in particular, the impingement of O⁻ ions with kinetic energies between 20 and 200 eV. Overall, it is also demonstrated that there are two microstructuring regimes in the growth of amorphous SiO₂ thin films by magnetron sputtering at low temperatures, which stem from the competition between surface shadowing and ion-induced adatom surface mobility.

*** Corresponding author:**

D. Manuel Macías Montero

Email: manuel.macias@icmse.csic.es

Nanoestructuración de Láminas Magnéticas mediante Copolímeros en Bloque Auto-Organizados

F. Valdés-Bango^{1,3}, F.J. García Alonso^{2,3}, G. Rodríguez-Rodríguez^{1,3}, L. Morán Fernández²,
J.I. Martín^{1,3*}, J.M. Alameda^{1,3}

¹Depto de Física, Univ. Oviedo, C/ Calvo Sotelo s/n, 33007, Oviedo, Spain.

²Depto. de Química Inorgánica, Univ. Oviedo, Av Julián Clavería nº8, 33006, Oviedo, Spain.

³Centro de Investigación de Nanomateriales y Nanotecnología-CINN (CSIC-Universidad de Oviedo-Principado de Asturias) Parque Tecnológico de Asturias, 33428 Llanera, Spain.

ji.martin@cinn.es

Las técnicas litográficas bottom-up han generado un gran interés en los últimos años debido a un mayor control creciente y la versatilidad de las mismas [1]. Particularmente, los materiales auto-organizados, capaces de segregarse en redes de fases nanoestructuradas en grandes áreas, está logrando grandes progresos en áreas tan diversas como la biomédica (biosensores), en óptica (láseres o pantallas de cristal líquido), para memorias orgánicas,...

En este experimento, se ha realizado un estudio de la optimización en los procesos de obtención de estructuras ordenadas del copolímero en bloque auto-organizado (Poliestireno) – b - (Poli-4-Vinilpiridina) (PS-P4VP), sobre láminas delgadas de Si (100), mediante procesos de spin-coating de disoluciones del mismo, con el objetivo de usarlas para la creación de redes de puntos magnéticos, y servir como buffer de muestras magnéticas. Se ha logrado que dicho material se disponga en una red hexagonal en una estructura micelar de PS-P4VP (Shell-Core). Después, mediante exposición química y ataque con iones de oxígeno reactivos (RIE) se genera una máscara que puede emplearse bien para el crecimiento de una red ordenada de puntos magnéticos nanométricos (agujeros de diámetro base ~40-50nm, espesor ~3-10nm, ver Fig1), o bien como buffer de crecimiento de láminas delgadas magnéticas (en nuestro caso de la aleación $Nd_{16}Co_{84}$ amorfa con una fuerte anisotropía magnética perpendicular [2]). Se crecieron láminas delgadas de Nd-Co de distintos espesores (40 y 60 nm) mediante sputtering magnetrón sobre los buffer de copolímero y, posteriormente, se caracterizaron magnéticamente mediante efecto magneto-óptico Kerr transversal (MOTKE). Los resultados evidenciaron un cambio notable en los ciclos de histéresis presentados por las muestras (ver Fig 2), favoreciendo la orientación de la imanación en el plano de las láminas y, por tanto, modulando la anisotropía magnética efectiva de las mismas.

[1] E.Huang et al, *Macromolecules* 31 (1998) 76417

[2] R. Cid et al, *J. Magn.Magn.Mat.* 316 (2007) 446.

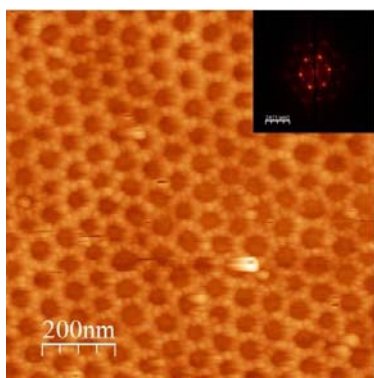


Fig1: Máscara nanoporosa de PS-P4VP.

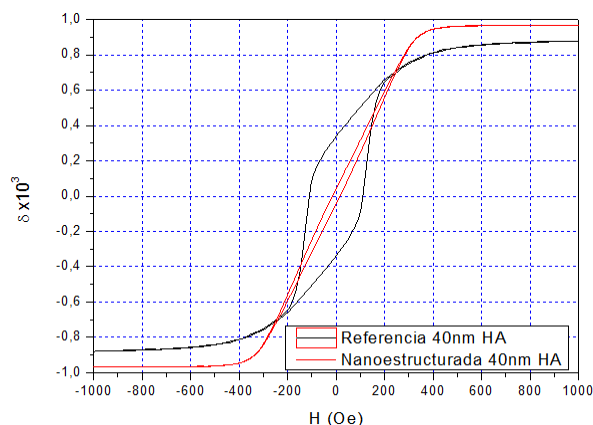


Fig2: Ciclo de histéresis con y sin buffer de PS-P4VP.

Oriented epitaxial growth of ferromagnetic LaSr-2x4 manganese oxide molecular sieve nanowires

Adrián Carretero-Genevri¹, Jaume Gázquez^{1,2}, César Magén³, J. Oro¹, María Varela², Etienne Ferain⁴, Teresa Puig¹, Narcís Mestres^{1*}, and Xavier Obradors¹

¹Institut de Ciència de Materials de Barcelona ICMAB, Consejo Superior de Investigaciones Científicas CSIC, Campus UAB 08193 Bellaterra, Catalonia, Spain

²Materials Science and Technology Division, Oak Ridge National Laboratory, Oak Ridge, TN 37831, U.S.A.

³Instituto de Nanociencia de Aragón (INA), Universidad de Zaragoza, 50018 Zaragoza, Spain

⁴Institute of Condensed Matter and Nanosciences, Bio & Soft Matter (IMCN/BSMA), Université catholique de Louvain, Croix du Sud 1, 1348 Louvain-la-Neuve, Belgium, and it4ip s.a., rue J. Bordet (Z.I. C), 7180 Seneffe, Belgium

We report a chemical solution based method using nanoporous track-etched polymer templates supported on top of single crystalline substrates for producing LaSr-2x4 manganese oxide monoclinic molecular sieve nanowires. Due to the confined nucleation in high aspect ratio nanopores and to the high temperatures attained, new structures with novel physical properties have been produced. During the calcination process, the nucleation and crystallization of ϵ -MnO₂ nanoparticles with a new hexagonal structure is promoted. On Silicon substrates, these nanoparticles generated up to 30 μ m long and flexible hexagonal nanowires at mild growth temperatures (T_g= 700 °C) as a consequence of the large crystallographic anisotropy of ϵ -MnO₂. The nanocrystallites of MnO₂ formed at low temperatures serve as seeds for the growth of LaSr-2x4 manganese oxide nanowires at growth temperatures above 800 °C, through the diffusion of La and Sr into the empty 1D-channels of ϵ -MnO₂, and with ordered arrangement of La³⁺ and Sr²⁺ cations inside the 1D-channels. These nanowires exhibit ferromagnetic ordering with strongly enhanced Curie temperature (T_c > 500 K) that probably results from the new crystallographic order and from the mixed valence of manganese [1].

In addition, epitaxial LaSr-2x4 nanowires self aligned along the <110> directions are obtained when the same methodology is used on the (001) surface of gadolinium-doped CeO₂. The growth of oriented long uniaxial nanostructures occurs due to the inherent highly anisotropic structure of monoclinic LaSr-2x4 and to the relatively good epitaxial lattice match along the growth directions. These nanowires are extremely appealing as building blocks in future spintronic devices.

[1] A. Carretero-Genevri *et al.*, Journal of the American Chemical Society 133, (2011) 453

Co-ferrite nanoparticles with spin- glass- like

C. Moya¹, N. Pérez¹, X. Batlle¹, A. Labarta¹

¹ Departament de Física Fonamental and Institut de Nanociència i Nanotecnologia IN²UB, Universitat de Barcelona, Martí i Franqués 1, E-08028 Barcelona, Catalonia, Spain

Magnetic nanoparticles show a variety of unusual magnetic phenomenology when compared to the bulk materials, such as superparamagnetism, magnetic moment enhancement, oddly shaped hysteresis loops, and glassy behaviour¹. In addition, there might be a breakdown of the usual scaling laws linking magnetic properties to size. These effects are due to the influence of the surface on magnetic interactions via bond breaking and charge rearrangement, and to the closeness of the particle size to critical magnetic length scales such as the domain wall width and the exchange length². In the case of spinel ferrites such as $\text{Co}_x\text{Fe}_{2-x}\text{O}_4$, further complexity arises due to the likely size-dependent cation distribution of the tetrahedral and octahedral sites in the close-packed oxygen structure, which strongly affect the magnetic properties of the particles such as saturation magnetization and magnetic anisotropy .

In this work, we present the synthesis of Co-ferrite nanoparticles with a narrow size distribution by the high-temperature decomposition method of iron and cobalt organic precursors in an organic solvent³. The mean size of the nanoparticles can be modified with the reaction conditions. It is worth noting that nanoparticles 8 nm in size show spin glass-like behaviour at low temperature with strong magnetic frustration associated with highly defective crystallographic structure. The existence of a frozen disordered state at low temperature is supported by the observation of largely shifted hysteresis loops (exchange bias) after field cooling to 5 K in a 1 T field. Such a spin-glass-like freezing seems to develop throughout the entire volume of the nanoparticle, in contrast to earlier results by other authors who attribute a similar behaviour to the random freezing of surface spins⁴. Our high resolution transmission electron microscopy (HRTEM) measurements exclude the formation of a core-shell structure, and indicate the presence of crystallographic defects and/or domain boundaries inside the nanoparticles, giving rise to a strong magnetic frustration which is responsible of the formation of spin-glass-like regions between ferrimagnetically ordered spins (core of the crystallographic domains). Above the freezing temperature, the nanoparticles undergo an unblocking process towards a typical SPM regime where the magnetization curves at different temperatures can be scaled in a conventional H/T plot. As the particle size increases to 12 nm, the ferrimagnetic (FiM) contribution to the hysteresis loop becomes increasingly more predominant, even at low temperatures. This could be related to the presence of fewer defects and cation vacancies, or to an enhanced structural relaxation compared to the smaller particles.

¹X. Batlle and A. Labarta *J. Phys. D: Appl. Phys.* **35** R15 (2002).

²J. Bansmann et al, *Surf. Sci. Rep.* **56** 189 (2005).

³N. Pérez, F. López-Calahorra, A. Labarta, and X. Batlle, *Physical Chemistry Chemical Physics* **3** 19485 (2011).

⁴D. Peddis, C. Cannas, G. Piccaluga, E. Agostinelli, and D. Fiorani, *Nanotechnology* **21** 15705 (2010).

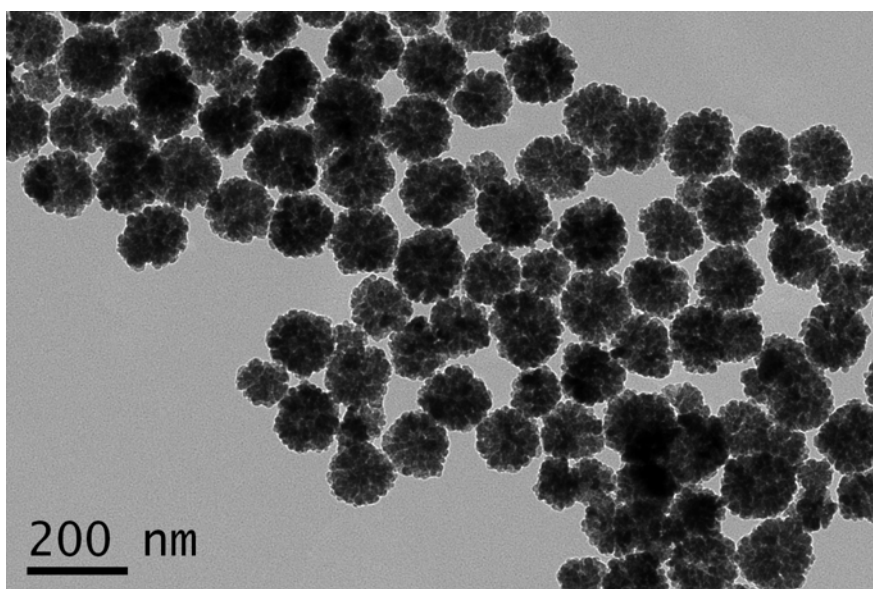
Synthesis of magnetic composites through controlled aggregation of nanoparticles using an autoclave system

Ruth Otero Lorenzo,* Sara Liébana Viñas, Verónica Salgueiriño

¹Universidade de Vigo, Department of Applied Physics, 36310 Vigo, Spain

We propose the controlled aggregation of magnetite nanoparticles using an autoclave system. The chemistry involved permits to control the size of the magnetite units to aggregate into the final clusters, with the consequent ability to control the collective magnetic behavior.

This assembly can also help to enhance the possible diversity of the ultimate functionalities of these complex nanomaterial systems, in view of the possible interfaces established. This fascinating approach of artificial nanostructuring permits to develop mix multifunctional systems, driving besides magnetite, gold nanoparticles that favor the acquisition of a characteristic surface plasmon band, or depositing a chromium oxide outer shell, favoring a ferrimagnetic-antiferromagnetic interface. [1]



[1] Sara Liébana Viñas, Ruth Otero Lorenzo, Verónica Salgueiriño, (2011) in preparation.

Light controlled patterning of ONWs on ITO and TiO₂ Surfaces

Y. Oulad-Zian,^{*} J. R. Sanchez-Valencia, A. Borrás, A. R. Gonzalez-Elipé and J. P. Espinos

¹Instituto de Ciencia de Materiales de Sevilla (ICMS, CSIC-US), Nanotechnology on Surfaces Lab., C/ Américo Vespucio 49, 41092, Sevilla, Spain.
Switzerland

In this communication we show the basis of a light controlled patterning formation of organic nanowires (ONWs). In previous references¹ we have report on the vacuum fabrication of ONWs based on π conjugated molecules on different substrates. Thus, supported single crystal ONWs of metal porphyrins (PdOEP, PtOEP), metal phthalocyanines (CuPc, CoPc, FePc) and perylenes (MePTCDI) grow at low temperature on metal and oxide substrates of tailored surface roughness. Herein we focus on the patterning formation of PdOEP NWs on porous TiO₂ thin films. Thus we present the effect on the UV light irradiation of this wide band gap semiconductor on the controlled formation either of hybrid thin films (PdOEP filling the porous structure of the TiO₂ film) or high density arrays of ONWs supported on the film surface. Hybrid materials and ONWs were characterized by SEM, UV-Vis absorbance and fluorescence. Moreover, in situ XPS experiments were carried out in order to fully describe the mobility of the organic molecules on the porous structure.

[1] A. Borrás, M. Aguirre, O. Groening, C. Lopez-Cartes, P. Groening, Chem. Mater. 2008, 20, 7371.

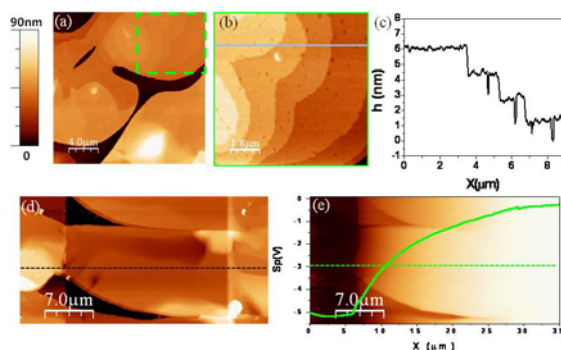
Multi-scale approach correlation between structure and properties of diF-TES ADT Organic Thin Film Transistors

Markos Paradinas^{1,*}, Mariona Coll¹, Esther Barrena¹, Oana D. Jurchescu² and Carmen Ocal¹

¹*Instituto de Ciència de Materials de Barcelona (ICMAB-CSIC)
Bellaterra 08193, Barcelona, Spain*

²*Department of Physics, Wake Forest University, Winston-Salem, NC 27109, USA
E-mail: mparadinas@icmab.es*

The performance of Organic Thin-Film Transistors (OTFTs) is often strongly dependent on the morphological conformation of the molecular films across the transistor channel [1]. Structural defects as grain-boundaries can significantly affect the local transport properties [2] yielding to a drop on the device operation properties. In this work, the influence of structural defects in the device performance is studied by the correlation of micro-scale characteristics with the nano-scale morphological and electronic properties. A combination of different Scanning Force Microscopy (SFM) is proposed to in-situ provide such correlation of the OTFT operating channel obtained by Kelvin Probe Force Microscopy (KPFM) and Conductive Scanning Force Microscopy (CSFM). The obtained results will be discussed in terms of voltage threshold, contact resistance, carriers' mobility as well as possible charge trapping mechanisms and stress bias effects.



The influence of crystalline order and structural features, (as the grain boundaries, steps or vacancies shown in (a-c) for a diF-TES ADT film [3]) can be directly correlated to the position-dependent potential drop within the channel if measured simultaneously (d-e)

during operation, i.e. as a function of V_{DS} and V_{GS} . Moreover, the electrical transport trough each individual defect can be obtained by measuring the electronic current flowing from the source to the C-SFM tip, acting as a movable drain located at different distances from the source.

- [1] L. C. Teague, B. H. Hamadani, O. D. Jurchescu, S. Subramanian, J. E. Anthony, T. N. Jackson, C. A. Richter, D. J. Gundlach, and J. G. Kushmerick, *Advanced Materials* **20** (23), 4513 (2008).
- [2] T. W. Kelley and C. D. Frisbie, *The Journal of Physical Chemistry B* **105** (20), 4538 (2001).
- [3] J.W. Owen, N.A. Azarova, M.A. Loth, M. Paradinas, M. Coll, C. Ocal, J.E. Anthony, and O.D. Jurchescu. *Materials and Devices for Organic Electronics* issue of *Journal of Nanotechnology* Volume 2011, Article ID 914510 (2011)

Very fast growth of functional oxide thin-films and nanostructures prepared by Chemical Solution Deposition

A. Queraltó*, A. Pérez del Pino, T. Puig, X. Obradors

Materials Science Institute of Barcelona (ICMAB-CSIC), Department of Superconducting Materials and Large Scale Nanostructures, Campus UAB, 08193 Bellaterra, Spain

Chemical Solution Deposition (CSD) is a powerful bottom-up, scalable and low-cost approach to get very homogeneous thin-films and uniformly distributed nanostructures of confined sizes and appointed orientations. Conventional Thermal Annealing (CTA) used in CSD is prohibitive for industrialization processes due to long processing times. We propose two new promising growing strategies: Rapid Thermal Annealing (RTA) and Pulsed-Laser Annealing (PLA), with very different processing times and so, different nucleation kinetics.

We have grown oxide thin-films and nanostructures of doped cerium oxide, lanthanum strontium manganite and barium strontium titanate on different substrates like YSZ, STO (SrTiO₃), LAO (LaAlO₃) or metallic tapes.

For PLA case, we used a Nd-YAG laser ($\lambda=266$ nm, 10 Hz) in air to process metalorganic films. Temperature simulations using COMSOL Multiphysics software let us select proper fluences to control different regimes and obtain crystalline films. We used either samples pyrolyzed using a hot-plate at 300°C during 15 min or pyrolyzed by laser at low fluences. Decomposition process was controlled using an FTIR spectrometer, analyzing the disappearance of the carboxylic band. At high fluences crystallization proceeds. XRD analysis confirms epitaxial film growth in 1 μ s/pulse of accumulated time. The homogeneity of these films was studied by AFM with roughness of 1-5 nm.

For RTA case, we mainly investigated the formation of gadolinium-doped cerium oxide (CGO) self-assembled nanostructures.

In particular, we studied nucleation, growth and kinetic processes of different CGO heteroepitaxies depositing diluted solutions on LAO (001) and (011) substrates. The nucleation stage has been studied using RTA processes and the subsequent nuclei growth evolution has been further investigated using CTA. Heating ramps, oxygen partial pressure and growth temperature were varied to stabilize different orientations. Specifically, we studied the formation of (001)CGO nanodots of 2-8 nm height and equivalent diameter below 50 nm; (001) and (011)CGO nanowires of 4-16 nm height, 40 nm width and length from hundreds of nanometers to several micrometers.

Thermodynamic analyses were used to model different shapes observed, considering the role of modified biaxial strain. The equilibrium shape of (001)CGO nanoislands corresponds to square-based nanopyramids. Instead, (011)CGO nanowires have a square-based pyramid shape with an elongated direction.

Observation of ferroelectric domains in lead free piezoelectric materials by confocal Raman microscopy

J.J. Romero^{1,*}, F. Rubio-Marcos¹, A. del Campo¹, J.F. Fernandez¹

¹Instituto de Cerámica y Vidrio, CSIC, C/Kelsen 5, 28049-Madrid, Spain

Ferroelectric domains are usually observed by chemically etching the ferroelectric material, due to the different etching speed presented by the surface of domains with different polarization direction. This technique, though easy and well established, is a destructive technique, fixing the domains distribution present at the moment of the chemical etching.

Since its discovery in 1930, Raman spectroscopy has revealed many applications on materials characterization. This technique measures the characteristic vibrations of the atomic bonds, and can then be considered as material specific. In crystalline materials, Raman is also sensitive to very small variations of the crystal lattice, being then a fast and reliable technique for the study of material's stress and phase transitions. Moreover, it has been recently shown that Raman spectra can be used as an indicative of the polarizability of materials [1].

Nowadays, Confocal Raman Microscopy (CRM) has emerged as a very powerful characterization technique, capable of study materials' properties with a spatial resolution about one quarter of a micron. This technique combines the excellent characterization capabilities of the Raman spectroscopy with the spatial resolution of the confocal microscopy.

In this work, we obtain images of the ferroelectric domains of two families of lead-free piezoelectric materials: BaTiO₃ and modified-KNN. Since CRM is a non-destructive technique, it is possible to obtain images of the ferroelectric domains under different applied electric fields and/or different temperatures, making then dynamic studies of the ferroelectric domains movements possible.

[1] F. Rubio- Marcos, M. A. Bañares, J.J. Romero, J. F. Fernandez, *J. Raman Spectrosc.* **42**, 639–643 (2011)

Influencia de las interacciones entre fases en el efecto magnetocalórico de composites

C. Romero-Muñiz^{1,*}, V. Franco¹, A. Conde¹

¹Dpto. Física de la Materia Condensada, ICMSE-CSIC, Universidad de Sevilla. Apdo. 1065. 41080-Sevilla, España

Recientemente se está tratando de sustituir la refrigeración basada en la compresión y expansión de gases por sistemas de refrigeración magnética basados en el efecto magnetocalórico. Esto se debe a la mayor eficiencia energética de este tipo de dispositivos y a su mayor respeto al medio ambiente, puesto que al tratarse de refrigeración de estado sólido, no usan compuestos volátiles que afecten a la capa de ozono o produzcan efecto invernadero.

La optimización de la respuesta magnetocalórica de los materiales magnéticos se puede abordar de dos maneras distintas. La primera de ellas es la búsqueda de nuevos compuestos y aleaciones que permitan incrementar la variación de temperatura adiabática y la capacidad de refrigeración de los mismos. Sin embargo, la gran cantidad de grupos de investigación trabajando en este tema en los últimos años hace prever que las posibilidades de descubrir un nuevo compuesto con una respuesta notablemente distinta a los estudiados previamente sea cada vez más remota. Una aproximación alternativa es el uso de técnicas de ingeniería de materiales: emplear materiales bien conocidos para la fabricación de materiales multifásicos y composites que nos permitan aumentar la capacidad de refrigeración.

Estudios previos han puesto de manifiesto que mediante la fabricación de composites se pueden obtener capacidades de refrigeración casi un 90 % mayores que las de los materiales de partida [1]. Sin embargo, las simulaciones realizadas hasta el momento no contemplan la posibilidad de interacciones entre las fases. En este trabajo se analiza la influencia de las interacciones magnéticas entre las fases, introducidas mediante un modelo de campo medio, sobre la respuesta magnetocalórica de los composites, poniendo de manifiesto las regiones óptimas de comportamiento de estos materiales.

Este trabajo ha sido financiado por el Ministerio de Ciencia e Innovación y EU FEDER (Proyecto MAT 2010-20537), el PAI de la Junta de Andalucía (Proyecto FQM-6462), y la United States Office of Naval Research (Proyecto N00014-11-1-0311).

[1] R. Caballero-Flores, V. Franco, A. Conde, K. E. Knippling, and M. A. Willard. Appl. Phys. Lett. 98 (2011) 102505

Mechanochemistry as a method for the synthesis of multiferroic materials

A.Perejón¹, P.E. Sánchez-Jiménez^{1,*}, M.J. Diánez¹, J.M. Criado¹, L.A. Pérez-Maqueda¹

¹Instituto de Ciencia de Materiales de Sevilla (CSIC-Univ. Sevilla) 41092 Sevilla, Spain.

Magnetoelectric materials are those which present an induction of the magnetization by the effect of an electric field or the polarization by a magnetic field. Hence, these materials belong to the family of multiferroics and show a coexistence of ferroelectric and magnetic ordering. Thus, due to its physical properties, magnetoelectrics could be used either as ferroelectrics or as magnetic materials in devices for data storage, spintronics, sensors, etc.

BiFeO₃ features magnetoelectricity at room temperature, making it one of the most studied multiferroics. Many synthesis methods has been proposed to obtain a pure phase in bulk of BiFeO₃, i.e. solid state reactions, wet chemical synthesis including sol-gel methods starting from polymeric precursors, solution combustion methods, mechanical activation, hydrothermal synthesis, etc, but in most of cases small amounts of impurity phases, that damages the physical properties of this material, are present.

In this work, a mechanochemical approach has been used for obtaining a pure phase of BiFeO₃. This is a general, simple and reproducible method to synthesize BiFeO₃ starting from stoichiometric amounts of Bi₂O₃ and Fe₂O₃. Here, the experimental conditions used to prepare this material are presented and, additionally, the mechanism of the reaction between the starting oxides is clarified. The comprehension of this mechanism is very important in order to optimize the milling conditions.

The resulting materials have been characterized in terms of their structure, microstructure and physical properties using different experimental techniques such as X-ray powder diffraction, high temperature differential scanning calorimetry, electron microscopy, dilatometry and dielectric spectroscopy.

Effect of cationic order and origin of the dielectric anomalies in $\text{La}_2\text{MnCoO}_6$.

C. Frontera^{1,*}, A.J. Barón-González¹, J.L. García-Muñoz¹, B. Rivas-Murias², J. Blasco³

¹Instituto de Ciencia de Materiales de Barcelona, ICMAB-CSIC, Campus Universitario de Bellaterra, 08193 Bellaterra, España.

²Universidad de Santiago de Compostela, Departamento de Química-Física y Centro de Investigación en Biología Química y Materiales Moleculares, Santiago de Compostela, España.

³Instituto de Ciencia de Materiales de Aragón, ICMA-CSIC, c/ Pedro Cerbuna 12, E-50009 Zaragoza, España

We have prepared and deeply characterized two different bulk samples of $\text{La}_2\text{MnCoO}_6$ double perovskite. By varying the cooling rate after the final sintering temperature, we have got two different degrees of Mn/Co order (defined as the amount of Co or Mn in the corresponding crystallographic sublattice): 95 and 74%. Magnetic properties, structural behavior, dielectric anomalies and magnetodielectric response of $\text{La}_2\text{MnCoO}_6$ have been investigated by means of ultra-high resolution synchrotron X-ray powder diffraction, neutron powder diffraction (used to determine the degree of cationic order), resistivity, magnetization, and dielectric measurements.

Both samples present a clean and sharp transition from a paramagnetic (PM) to a ferromagnetic (FM) state on cooling. Beside the well known influence on magnetic properties, our results show that the main effect of disorder lies on the electrical resistivity.

Bond distances clearly show $\text{Mn}^{4+}/\text{Co}^{2+}$ valence states in well ordered sample and that these valences do not change across PM to FM transition. For the disordered one, this picture is compatible with experimental results.

Ultra high-resolution synchrotron X-ray powder diffraction demonstrates that PM to FM transition takes place with no magnetostriction effect, in contrast with other double perovskites showing dielectric anomalies.

AC-data evidence dielectric anomalies and a small magnetodielectric effect, but impedance complex plane analyses prove that these phenomena appear at the frequency-temperature region where extrinsic effects dominate the dielectric response.

Ab-Initio calculations including Van der Waals interactions: the SnS₂ layered material.Y. Seminóvski^{1,*}, P. Palacios^{1,2}, R. Grau-Crespo³, P. Wahnón¹¹Universidad Politécnica de Madrid, Grupo de Cálculos Cuánticos, ETSI Telecomunicación, Ciudad Universitaria s/n. C.P. 28040 Madrid, Spain² Universidad Politecnica de Madrid, Dpt. FQAT Aeronautica, Ciudad Universitaria, 28040, Madrid, Spain³Christopher Ingold Laboratories 20 Gordon Street, London WC1H 0AJ, United Kingdom

Tin disulfide SnS₂ was recently proposed as a high efficiency solar cell precursor [1]. The aim of this work is a deep study of the structural disposition of the most important polytypes of this layered material, not only describing the electronic correlation but also the interatomic Van der Waals interactions that is present between the layers.

The two recent implementations to take Van der Waals interactions into account in the VASP code are the self-consistent Dion *et al.* [2] functional optimized for solids by Michaelides *et al* [3] and the Grimme [4] dispersion correction that is applied after each autoconsistent PBE electronic calculation.

In this work these two methods are compared with DFT PBE functional. The results we will presented at this Conference, demonstrates the enhancement of the geometric parameters by the use of the Van der Waals interactions in agreement with the experimental values.

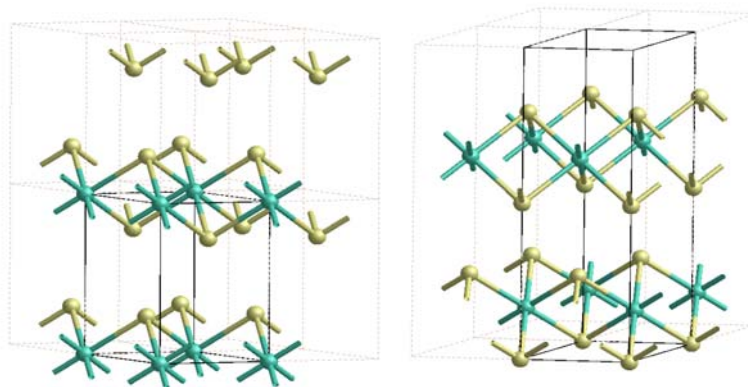


Fig. 1- SnS₂ polytypes a) SnS₂-2H b) SnS₂-4H

[1] P. Wahnón et al, Phys. Chem. Chem. Phys., 2011, **13**, 20401-20407

[2] M. Dion, H. Rydberg, E. Schröder, D. C. Langreth, and B. I. Lundqvist, Phys. Rev. Lett. **92**, 246401 (2004).

[3] J. Klimeš, D. R. Bowler, and A. Michaelides, Phys. Rev. B **83**, 195131 (2011).

[4] S. Grimme, J. Comp. Chem. **27**, 1787 (2006).